Lawrence Berkeley National Laboratory
Recent Work

Title
Dynamic Observation of Interface Motion During the Oxidation of Silicon

Permalink
https://escholarship.org/uc/item/96t3s7j3

Journal
Surface Science, 310

Authors
Ross, F.M.
Gibson, J.M.
Twesten, R.D.

Publication Date
1993-07-01

eScholarship.org Powered by the California Digital Library
University of California

LBL-34392
UC-404
Preprint

Lawrence Berkeley Laboratory

UNIVERSITY OF CALIFORNIA

Materials Sciences Division

National Center for Electron Microscopy

Submitted to Surface Science

Dynamic Observations of Interface Motion During the Oxidation of Silicon

F.M. Ross, J.M. Gibson, and R.D. Twesten

July 1993

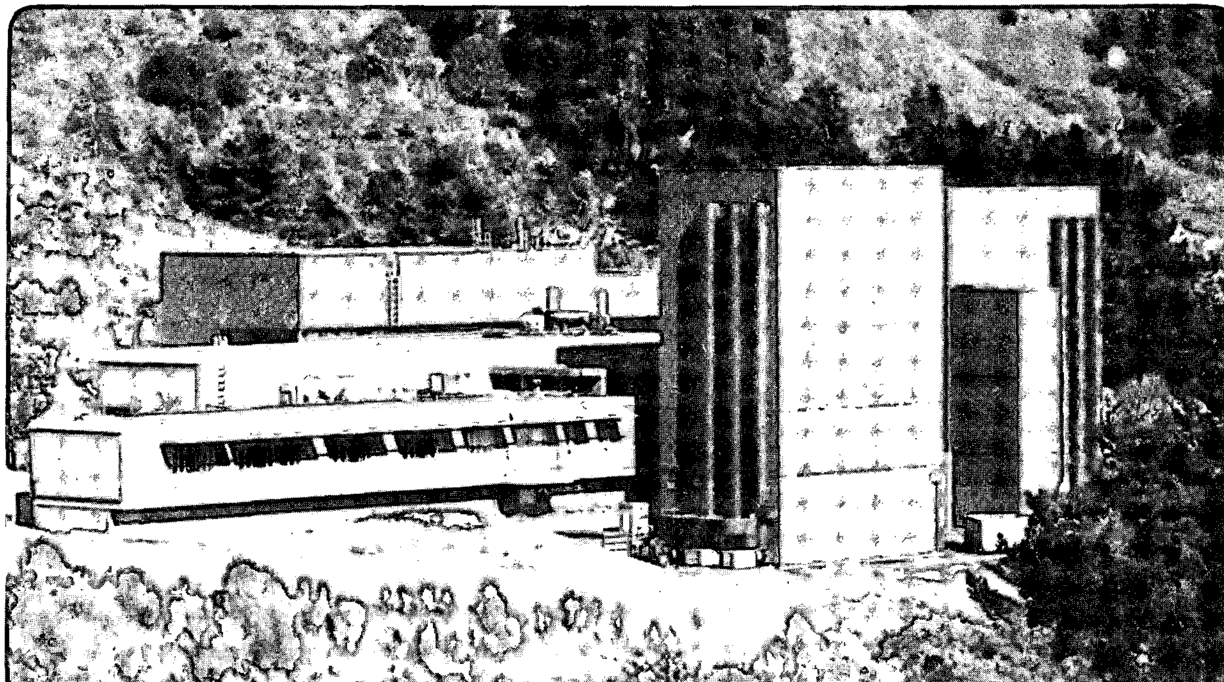

LOAN COPY
Circulates
for 4 weeks
Bldg. 50 Library.
Copy 2
LBL-34392

Prepared for the U.S. Department of Energy under Contract Number DE-AC03-76SF00098

DISCLAIMER

This document was prepared as an account of work sponsored by the United States Government. While this document is believed to contain correct information, neither the United States Government nor any agency thereof, nor the Regents of the University of California, nor any of their employees, makes any warranty, express or implied, or assumes any legal responsibility for the accuracy, completeness, or usefulness of any information, apparatus, product, or process disclosed, or represents that its use would not infringe privately owned rights. Reference herein to any specific commercial product, process, or service by its trade name, trademark, manufacturer, or otherwise, does not necessarily constitute or imply its endorsement, recommendation, or favoring by the United States Government or any agency thereof, or the Regents of the University of California. The views and opinions of authors expressed herein do not necessarily state or reflect those of the United States Government or any agency thereof or the Regents of the University of California.

LBL-34392

Dynamic Observations of Interface Motion During the Oxidation of Silicon

F.M. Ross, J.M. Gibson* and R.D. Twesten*

Materials Science Division
National Center for Electron Microscopy
Lawrence Berkeley Laboratory
University of California, Berkeley, CA 94720

*University of Illinois
Materials Research Lab
104 S. Goodwin Avenue
Urbana, IL 61801

Submitted to the Journal of Surface Science (7/93)

This work was supported in part by the Director, Office of Energy Research, Office of Basic Energy Sciences, Materials Science Division of the U.S. Department of Energy under Contract No. DE-AC03-76SF00098 and University of Illinois Contract No. DE FG02-91ER45439.

Dynamic observations of interface motion during the oxidation of silicon

Frances M. Ross°, J. Murray Gibson*
AT&T Bell Laboratories, 600 Mountain Avenue, Murray Hill, NJ 07974, USA
° Present address: National Center for Electron Microscopy, Lawrence Berkeley Laboratory, 1 Cyclotron Road, Berkeley, CA 94720, USA
* Present address: University of Illinois Materials Research Laboratory, 104 S. Goodwin Avenue, Urbana, IL 61801, USA

and Ray D. Twesten
University of Illinois Materials Research Laboratory, 104 S. Goodwin Avenue, Urbana, IL 61801, USA

Abstract

We describe real time observations of the behaviour of the silicon - oxide interface during oxidation *in situ* in an ultra high vacuum transmission electron microscope. We have formed clean, flat Si (111) surfaces by heating under UHV and allowed oxidation or oxygen etching to proceed in the microscope. We have examined the kinetics of both the oxidation and etching reactions using an imaging technique based on the use of forbidden reflections in silicon. We find that oxidation to form SiO_2 occurs by the reaction of discrete monolayers with no flow of surface steps. This is in dramatic contrast to oxygen etching, during which the volatile oxide SiO evaporates preferentially from step edges.

Contact Author:
Frances M. Ross
National Center for Electron Microscopy,
Lawrence Berkeley Laboratory, Building 72-133
1 Cyclotron Road, Berkeley, CA 94720, USA

Phone (510) 486 5516; Fax (510) 486 5888; Electronic mail FMROSS@LBL.GOV

1. Introduction

The behaviour of the silicon surface during oxidation is of fundamental interest, both as a model system and because of the need to understand and control the formation of a defect-free silicon-oxide interface for electronics applications. We have therefore developed a technique which allows us to make observations, in real time, of the progressive changes occurring at a silicon surface when it is exposed to water vapour or oxygen. In this paper we present the results of this investigation. We describe the fascinating behaviour of the silicon surface as oxidation occurs and derive kinetic models for the oxidation reaction from our observations.

Silicon exhibits two types of oxidation reaction, firstly the formation of SiO_2 at low temperature and high oxygen pressure, and secondly an etching reaction, in which the volatile oxide SiO is formed, at higher temperature and lower pressure. To examine these reactions at the atomic level requires a technique capable of imaging surfaces and buried interfaces in real time over a wide range of temperatures and pressures. Our solution to this problem is to allow oxidation to take place *in situ* in a UHV transmission electron microscope after forming clean, flat Si (111) surfaces under UHV. To visualise the changes occurring during oxidation we use an imaging technique based on the behaviour of forbidden reflections in silicon. This technique can resolve step and terrace configurations even when the interface is buried under an oxide film, and we can therefore follow oxidation reactions beyond the first monolayer. Analysis of electron diffraction patterns provides complementary information about atomic structure at both buried interfaces and free surfaces. These two techniques enable us to make quantitative measurements of the behaviour and movement of surface and interface steps and terraces during the oxidation reaction.

We find that the behaviour of steps and terraces is a sensitive probe of the mechanism of the oxidation reaction. In this paper we will show that surface steps, which are two monolayers (0.31nm) in height, *do not move* visibly during oxidation induced by the electron beam at low pressure and temperature, during native oxidation at atmospheric pressure, or during high temperature thermal oxidation. This result, together with analysis of the changes in appearance of the terraces, demonstrates that oxidation is a terrace-attacking process and suggests that it occurs one monolayer at a time, with each monolayer reacting completely before the next is attacked. In contrast, step flow does occur during the etching reaction. We deduce a mechanism which again involves oxygen reaction on the terraces, but with preferential evaporation of SiO from step edges.

We will firstly describe the general oxidation and etching behaviour of silicon and the theory behind the forbidden reflection imaging technique we have used. Quantitative measurements can be made by comparing experimental images with computer simulations, in the same way as is done for high resolution electron microscopy. We describe the configuration of the initial silicon surfaces prepared under UHV in our microscope and the kinetics of both the oxidation and etching reactions, considering in particular, because of its great importance, the change in surface and

interface morphology which occurs during these reactions. We discuss the implications of our results for currently held beliefs concerning the oxidation reaction, in particular on the diffusion of silicon interstitials through a reactive layer at the silicon-oxide interface, and we present a kinetic model for oxygen etching. Some of these results have been summarised elsewhere [1].

2. The oxidation behaviour of silicon in oxygen and water vapour

It is known that a clean silicon surface can be either oxidised or etched by oxygen depending on the oxygen pressure and temperature [2, 3]. Oxidation to form SiO_2 takes place at high pressures, whereas oxygen etching, resulting from the reaction of Si and O_2 to form the volatile oxide SiO, takes place at lower pressures and higher temperatures. Previous studies have focused on the macroscopic equilibrium between these two reactions and have demonstrated that the behaviour of the $Si+O_2$ system depends on the balance between the arrival rate of oxygen and the rate at which SiO evaporates from the surface. This suggests a straight line boundary between the oxidation and etching régimes, as is found experimentally in $p \rightarrow {}^{1}/_{T}$ plots [2, 3].

We have observed both the oxidation and etching reactions at the Si(111) surface in a UHV electron microscope over a range of temperature and pressure. An overview of these results is shown in figure 1. The two reactions are easily distinguished in our system. The etching reaction proceeds by the movement of steps on the surface of the Si specimen, and in diffraction we see a Si 1x1 or 7x7 pattern, depending on whether the specimen is above or below the 7x7→1x1 transition temperature of 860°C. (We find that the 7x7→1x1 transition does not appear to affect the oxidation-etching boundary.) The oxidation reaction is characterised by a fading of the 7x7 pattern and a change in the intensity levels of terraces at the silicon-oxide interface, but we observe no movement of interface steps. We show below that these terrace intensity changes arise from the transformation of individual planes of silicon into amorphous SiO_2. In water vapour we see basically the same behaviour as for oxygen, although oxidation occurs at an enhanced rate.

Over an intermediate, limited range of pressure and temperature we also observe a "roughening reaction", characterised by unusual ringlike features in the diffraction pattern and a mottled rough appearance in dark field images. The macroscopic models described above do not suggest any transition region between the oxidation and etching régimes. However we believe that the condition of the surface strongly influences the reaction and we will discuss the relationship of surface morphology, defects and cleanliness to this transition régime in more detail below.

3. Dynamical observations of surface reactions *in situ*

Etching and oxidation experiments were carried out in a 200kV JEOL 200CX transmission electron microscope which had been modified to achieve a base vacuum in the region of the specimen in the high 10^{-9} Torr range, using a cryopump and turbomolecular pumping system [4].

The main contaminants in the vacuum system were H_2O and N_2. Gas inlet valves were added near the specimen area, allowing oxygen and water vapour to be leaked in to a pressure measured by a quadrupole mass analyzer. Differential pumping ensured that the electron beam could remain on while pressures of up to $5x10^{-4}$ Torr were maintained in the specimen area. Higher pressure oxidation experiments were also carried out (with the beam off) by allowing 1atm. of oxygen into the microscope column. The specimen holder, a non-tilting top entry design, was modified to enable direct resistive heating of the Si specimen up to its melting point, both for cleaning the surface prior to oxidation and for maintaining an elevated temperature during reactions. The specimen temperature was determined from the power dissipated using an equation which takes radiative losses into account. This equation was calibrated by pyrometry and values quoted are accurate to better than ±50°C.

Specimens were cut from (111) oriented p-doped 10 Ωcm silicon wafers and were mechanically dimpled and chemically prethinned. They were then heated *in situ* to about 1200°C. At this temperature, the surface oxide desorbed and the surface flowed to create locally thin areas with clean surfaces, separated by a thicker bead from the original specimen edge. Once a suitably thin (less than about 200nm), clean area was formed, surface sensitive information was obtained by analysis of electrons transmitted through the foil. Our analysis relies on the fact that, because of their altered structure, atomic planes near the surface scatter electrons differently from planes in the bulk. By either recording diffraction patterns or forming images with surface sensitive reflections, we are able to obtain information about the altered layers at surfaces and buried interfaces, even though most of the scattering takes place in the bulk. Figure 2 gives examples of a diffraction pattern showing surface sensitive reflections and images formed from one of these reflections. We will demonstrate below that the changes in grey level in figures 2b and 2c represent the positions of bilayer steps on either surface of the specimen; these steps are of height 0.31nm and spaced up to 1μm apart and they are separated by atomically flat terraces. Figure 2c also shows that the effect of carbon contamination in our system is to form epitaxial SiC particles at high temperatures. These have an interesting interaction with surface steps during step flow, as we will show below.

To monitor the progress of surface reactions in real time, the diffraction and imaging techniques shown in figure 2 provide complementary information. We firstly consider diffraction experiments. Two types of surface-sensitive diffraction spots appear in figure 2a, the 7x7 superlattice reflections and the more intense spots at the $^1/_3$ 422 positions. The $^1/_3$ 422 spots are bulk-forbidden surface reflections whose origin is discussed in more detail below; their intensities are typically about 10^{-3} - 10^{-4} of the incident intensity. The half-width of these reflections is a measure of the distance between surface or interface steps and has been used to determine the terrace widths of buried Si/SiO_2 interfaces without the need to etch away the covering oxide film [5]. The superlattice spots of course arise from the 7x7 reconstruction of the surface Si (111)

planes which is energetically favoured below 860°C. Their intensities are typically only about 10^{-5} of incident, but can be analysed quantitatively to yield both the initial configuration of the surface atoms, as was in fact originally done to solve the 7x7 structure [6], and the changes occurring after dosing with oxygen or water vapour. We have used this method to infer the sites at which oxygen first attacks the 7x7 structure, using an approach based on the analysis of Patterson functions [7]. The kinematical nature of high energy electron diffraction from monolayers makes this a very powerful technique. However, as the 7x7 structure becomes disordered, these superlattice spots fade and disappear. This can occur after oxygen doses as low as a few L ($1L=10^{-6}$ Torr sec.) under irradiation by the electron beam at room temperature [7]. To monitor progress beyond the first monolayer, we have therefore used a dark field imaging technique based on the use of the $^1/_3$ 422 reflections. In this method, the grey levels from images such as those in figure 2b and c are analysed by comparison with computer simulations to yield information about the configuration of terrace atoms at surfaces and buried interfaces.

We refer to images such as these as forbidden reflection (FB) images. Forbidden reflections, first discussed in detail by Cherns [8], have a structure factor of zero, in other words the bulk structure should not scatter any intensity into these positions. However, if there is a non-integral number of unit cells in the thickness of the specimen, some intensity can be seen because the incomplete fraction of a unit cell does not cancel all the amplitude in the reflection. As we demonstrate below, this gives FB images an important sensitivity to the configuration of the surface.

In the case of silicon in the (111) orientation, an appropriate bulk-forbidden reflection is indexed as $^1/_3$ 422 in the f.c.c. reciprocal lattice. The behaviour of the intensity in this reflection is best appreciated with reference to a hexagonal unit cell for silicon. This cell contains six atoms arranged in three pairs, with c=0.94nm along the cubic (111) direction (figure 3a). For a single unit cell, the six layers scatter out of phase yielding zero resultant intensity. This is shown schematically in figure 3b as a complete circuit around a triangle on an amplitude-phase diagram. The triangle is traversed many times within the thickness of a specimen but it is the relative positions of the start and end points which determine the final amplitude in the $^1/_3$ 422 reflection [8, 9, 10]. The scattered intensity is therefore a sensitive function of the number of atomic planes in the specimen, and the positions of surface steps are indicated in the images by changes in the background grey levels. This information is of course available even when the crystalline silicon is buried under another material with a different structure, such as amorphous SiO_2. This makes the technique extremely powerful for examining the configuration of the top planes of silicon atoms after oxidation has taken place. Intensity levels are great enough to allow video recording of the images using an image intensifier, and thus dynamical records of the changes in the surface or interface can be obtained.

As well as recording step positions, quantitative information about the configuration of the terraces can also be obtained from FB images by comparing the observed intensity levels with values calculated using simulations employing the multislice algorithm [11]. As we show below, these calculations demonstrate that the simple geometrical argument shown in figure 3b gives a reasonably accurate insight into the pattern of grey levels observed, although the presence of crystal tilt and other factors disrupt the symmetry of the diagram. However these calculations then enable us to go much further in making quantitative measurements of the atomic configuration of the silicon atoms on the terraces.

4. The morphology of UHV-prepared Si (111) surfaces

Silicon (111) surfaces prepared by heating under UHV show distinctive patterns of surface steps separated by terraces which are apparently atomically flat (figure 2b, c). Before dosing these surfaces with oxygen or water vapour, we analysed the intensity levels in FB images to characterise quantitatively the atomic configuration of the surface planes.

4.1 How high are the steps?

The simple argument given in figure 3b suggests that intensity levels in the $^{1}/_{3}$ 422 reflection should repeat themselves after a 6n monolayer (0.93n nm) change in specimen thickness. Although in general we can not determine which surface a given step is on, in some situations an echelon of parallel steps is clearly present on one surface while the other is flat. Figure 4 shows an example of this. For specimens of this type which are oriented close to the (111) zone we observe repeating contrast levels after every 3 steps. This offers direct proof that surface steps are two monolayers (2ML) high, i.e. 0.31nm. (4ML is a possible but unlikely alternative, which we rule out below by comparison with computer simulations.) Etching of well-oriented specimens by oxygen to expose successive terraces shows the same 3-fold repeat, and thus the units removed during etching are also 2ML in height.

Computer simulations, as we demonstrate in section 5.1, show that when the specimen is tilted further from the (111) zone we no longer expect an exact 3-fold repeat. Tilting the crystal modulates the intensity levels with an envelope function whose period depends on the tilt, leading to complicated intensity sequences with long repeat periods. We have observed these effects experimentally by examining the contrast levels of terraces removed during the etching reaction, which enables us to look at many more successive terraces (sometimes several hundred) than are normally available in a static field of view. For example, the complex series of intensity levels shown in figure 6 (section 5.1) is well predicted by models assuming that the surface steps are 2ML in height.

4.2 Shuffle or glide?

The removal of double rather than single monolayer steps makes sense on physical grounds. Depending on whether the crystal is cut between or within the pairs of planes shown in figure 3a, the exposed surface will have either one or three dangling bonds per atom. Above 860°C where no reconstruction occurs we label these two 1x1 surfaces the "shuffle" and "glide" terminations by analogy with dislocation theory. Removal of atomic planes in pairs will preserve whichever termination was present initially.

We expect these two types of surface to show different intensity levels in FB images, with the shuffle generally showing lower contrast. Although this is best demonstrated by carrying out multislice calculations, it can also be understood intuitively by considering figure 3b, where the glide terminations are represented by the vertices of the triangle and the shuffle by the midpoints of its edges, and hence a smaller amplitude. Multislice simulations show that a factor of approximately 2 in amplitude (4 in intensity) is indeed expected between glide and shuffle terminations. To distinguish these cases experimentally requires a comparison of terrace intensity levels with the incident intensity: unfortunately the small terrace size makes it difficult to isolate diffraction from a single terrace at a known specimen thickness. However, as mentioned above, for sufficiently high tilt (above about 5°) and a sufficiently long sequence of terraces, the symmetry is broken and the complicated patterns of contrast levels which arise are sufficiently distinctive to allow unambiguous identification of the shuffle termination (figure 6).

This conclusion is supported by evidence based on the comparison between the intensity levels of the known 7x7 structure and the 1x1 unreconstructed surface. Expected intensity levels for the 7x7 surface are midway between those of the shuffle and glide terminations (figure 3b; ref. [9]). On going from the 7x7 to the 1x1 structure, firstly by heating the 7x7 surface above 860°C and secondly by oxidising it, we see a decrease in contrast, suggesting that the 7x7 surface is transforming to the shuffle termination in both cases. The former experiment is a direct analogue of the beautiful low energy electron microscopy (LEEM) experiments carried out (at lower resolution) by Telieps and Bauer [12] and we observe similar nucleation and dynamics for the 7x7→1x1 transformation. Although the shuffle is the termination we might expect on physical grounds, it is interesting that a direct experimental verification of this fact is rather hard using other methods.

4.3 The 7x7 termination

As mentioned above, the intensities of superlattice reflections in a diffraction pattern can be used to analyse the atomic configuration of surfaces and buried interfaces. We have measured the intensities of the reflections obtained from 7x7 surfaces freshly prepared in our UHV system and compared them, using Patterson function analysis, with calculations from the expected 7x7 structure. Agreement is best for specimens which were firstly thinned to <20nm to reduce multiple scattering from the bulk by using the oxygen etching reaction [13]. We find that the as-prepared

surface is a good fit to calculations based on the DAS 7x7 model [6] if we add 50% occupancy of oxygen atoms to a single site on the 7x7 unit cell. This oxygen reaction is difficult to avoid in our system as it appears to occur extremely fast under irradiation by the electron beam, even for doses of <1L O_2; however the structure formed is stable to further doses of oxygen, without irradiation [7].

We conclude that the Si (111) surface prepared by heating under UHV is characterised by 2ML high surface steps separated by terraces up to several microns across. These terraces have the shuffle termination above 860°C, with one dangling bond per atom; at lower temperatures a slightly oxygen-contaminated 7x7 termination forms the initial surface for our subsequent oxidation experiments.

5 Oxygen Etching

5.1 Step flow during etching

The oxidation reaction $2Si+O_2 \rightarrow 2SiO$ occurs when a silicon surface is exposed to low pressures of oxygen at temperatures above about 800°C [2. 3]. The high vapour pressure of SiO results in its desorption from the surface, driving the reaction, and macroscopically we observe etching of the silicon specimen. A similar reaction also occurs during the high temperature cleaning of an oxidised silicon surface [2, 14], where the oxide acts as a source for the oxygen: $Si+SiO_2 \rightarrow 2SiO$. The mechanism of this reaction, and particularly the changes in surface morphology which occur during it, are therefore of interest in device processing.

In our system we observe the etching reaction when the specimen is at a temperature of 800-900°C and the oxygen or water vapour pressure is 10^{-7} - 10^{-4} Torr (figure 1). Microscopically, we observe that etching proceeds by the movement of bilayer steps on the surfaces of the specimen. Figure 5 shows a tracing of a step moving across a Si (111) surface during the etching process, taken from a video record of the experiment. It can be seen that steps flow smoothly unless obstructed by SiC particles. At lower temperatures, particularly below 860°C, the steps we see are more angular, preferring the lower energy <110> directions rather than flowing isotropically in the way shown here. Very low etching rates at lower temperatures can result in irregular etching and roughening of the step edges, particularly if the specimen surface is not very clean. We find it interesting that during etching below 860°C the 7x7 superlattice reflections remain visible in the diffraction pattern, indicating that the speed with which the surface reconstructs as each double layer is removed is greater than the speed of step movement, i.e. 1-10μm sec^{-1}.

It is possible to observe the intensity levels of a very long series of steps by allowing the etching reaction to proceed across a terrace such as that shown in figure 5. During one experiment which lasted 50 minutes we observed a sequence of 390 steps flowing across a thin area until the

silicon foil eventually etched through. We were able to record the intensity levels from video and match this line trace with computer simulations (figure 6). The good match between the pattern of grey levels for several hundred steps confirms that the steps are bilayer and shows that the terraces have the shuffle configuration, as discussed above.

5.2 The kinetics of step nucleation and step flow

In the experiment shown in figure 5, the point indicated acted as a nucleation site for steps, although an increasing proportion (up to 10%) nucleated at other points along the steep walls as the foil became thinner. We speculate that certain sites were preferred for nucleation because of strain effects caused by the abrupt change in specimen thickness. (In other experiments we observed steps nucleating from different points on both surfaces and passing across each other, in projection, without interacting.) Etching under these circumstances was limited by step nucleation, rather than by the speed at which the steps moved once formed. Quantitative observations of the dependence of both step nucleation rate and step velocity on the oxygen pressure during this experiment gave an insight into the mechanism of the etching reaction. We found that the nucleation rate (or the number of steps passing any point per second) was directly proportional to the oxygen pressure, while the step speed did not bear a simple relationship to pressure, increasing slowly with oxygen pressure above about 10^{-5} Torr but varying rapidly at lower pressures (figure 7).

These results suggest an oxidation mechanism for this reaction which is shown schematically in figure 8. We start with a stepped surface. Oxygen molecules impinge on the terraces and diffuse a certain distance before reacting to form Si-O bonds, presumably becoming comparatively immobile; subsequently evaporation of SiO occurs. The Si-O bonding reaction can occur either uniformly over the *terrace* (figure 8b) or preferentially at the *step edges* (figure 8a). We can distinguish these two scenarios because they predict different reaction kinetics. In the latter case the terraces play no role except in collecting oxygen over a strip one diffusion length wide along each step, making this scenario close to the spirit of crystal growth and evaporation models [16]. However, it predicts that step speed should be directly proportional to oxygen pressure (if oxygen supply is rate-limiting), which is not observed experimentally. It therefore appears that Si-O bonds are formed uniformly over the terraces. Even in this case the etching still proceeds by step movement, simply because evaporation of SiO is more likely to occur from a step edge than from the middle of a terrace (figure 8b). If no steps are present initially then nucleation must occur directly from the terrace by evaporation of SiO, a process which is likely to be rate limiting, as we observed in these experiments.

The linear relationship we observe between nucleation rate and p_{O2} suggests that step nucleation and flow requires a certain coverage of oxygen on the Si surface. This need not necessarily be a complete bilayer, but if it is, we can calculate from the oxygen flux a sticking

coefficient of 11±2% for oxygen molecules impinging on the surface. (In this calculation one O_2 molecule must react at each surface site since double layers are removed.) Similar calculations based on macroscopic measurements of the etching rate lead to results of the same magnitude at this temperature and range of pressures [2, 3, 17-19].

It thus appears that step nucleation and flow occurs once the surface is "activated" by a certain coverage of oxygen. We can not at present say what the chemical state of the oxygen is at this time, but we anticipate that analysis of diffraction patterns taken during etching below 860°C will yield information about where on the 7x7 structure the oxygen is first bonded [7]; this approach may also work above 860°C. The adsorption of O_2 on Si (111) has been examined by several spectroscopic techniques [20-22], although only at lower temperatures. Extrapolating these results to the temperatures at which we observe etching suggests that the reaction pathway in our experiments might proceed in two steps: firstly the formation of a molecular precursor consisting of a peroxy bridge formed by the reaction of an O_2 molecule with two dangling bonds, and secondly a state in which either one or both oxygen atoms have moved to bridging positions between Si atoms in the first and second layers. Oxygen bonded in the backbonds of the adatoms of the 7x7 structure has in fact been observed by STM [23, 24]. The peroxy bridge precursor, with one oxygen atom per surface site, has a short lifetime particularly at higher temperatures [22], decaying rapidly to the atomic bridging configuration. More oxygen can react at the second stage, increasing the oxygen coverage to the required two O atoms per surface Si site. From this latter configuration we can visualise how a step atom or part of the terrace, supplied with oxygen, can evaporate as SiO.

Given a fully reacted surface, preferential evaporation from step edges as we have suggested would lead to a step speed independent of the oxygen pressure, since all the oxygen required is already present bonded into the surface. As mentioned above, although there may be a limiting velocity at high pressure, at lower pressure we observe a strong pressure dependence. This slowing of the steps at lower pressures suggests that not all the oxygen required for step movement is readily available at the evaporating step edge, and that unreacted sites act as pinning points. It appears that some fraction of the oxygen must instead be supplied by diffusion from other parts of the terrace. The step will act as a sink for diffusing oxygen, so a concentration gradient will be set up around the step in the same way as is seen for adatom concentration during crystal growth according to the theory of Burton, Cabrera and Frank [16]. As in model 8a, this will lead to a step speed which is proportional to oxygen pressure. We suggest that this diffusion process controls the step speed at low pressures, but at higher pressures the rate limiting process is that determined by the evaporation kinetics. The combination of these two processes can produce a graph of the form shown in figure 7b. This explanation is only feasible if step nucleation and flow

can start at coverages of less than two monolayers; coverages between 1 and 2 monolayers are likely as soon as the peroxy bridge precursor reacts to form atomic bridging oxygen.

5.3 Changes in surface morphology during etching

The step flow mechanism which we have observed is important because it will clearly alter the silicon surface morphology. In our experiments, we find that the final morphology created by oxygen etching depends very strongly on both the initial configuration of the surface and its degree of cleanliness. Unlike the surface of a polished wafer, the regions we examine in these experiments typically have surface undulations on the scale of microns in height, and this morphology changes dramatically during etching. For example, the region shown in figure 5 was initially a small area at the bottom of a gently sloping valley, but as the etching proceeded the valley floor was flattened and enlarged with the walls becoming very steep. These changes in morphology suggest that the movement of steps is slowed at steep regions, i.e. by the presence of other steps nearby, a phenomenon consistent with theories of crystal growth to be discussed below. This results in preferential etching of smoother regions to give a potentially useful surface topography consisting of atomically flat terraces several microns across (larger for an initially flatter and cleaner surface) separated by steep walls. Sources of contamination such as SiC particles act as pinning sites for step movement. During step flow around these surface obstructions, the apparent size of the particles increases suggesting that they are left on the top of unetched cones of silicon of semi-angle about 60°.

We expect initially flatter, polished surfaces to etch in a different way. In the case of a vicinal surface, for example, all the steps should move regularly. If few steps are present initially we expect many simultaneous nucleation events from the middle of the terraces (as observed by REM; see below), increasing the degree of roughness. For such a flat surface the nucleation process is likely to be rate limiting, as we observed in these experiments. However, a surface which is initially very rough at the atomic scale is likely to be smoothed by the local movement of steps.

The same etching reaction occurs at the Si (100) surface and we have observed similarly smooth step flow. However we find that any degree of surface contamination which prevents free movement of steps leads to the formation of (111) facets during oxygen etching. A related observation is that roughening of the (100) surface can occur during desorption of a thick oxide [14]. Oxide decomposition, resulting in SiO formation, is initiated at existing defect sites, leading to the lateral growth of voids. Thus the (100) surface, unless initially very clean and oxide-free, is easily roughened by the etching reaction, so that it is important to avoid exposing it to pressures and temperatures in the etching régime.

The theory of Burton, Cabrera and Frank [14] applies to crystal growth only at low adatom supersaturations. We hope to use our observations of the shapes of surface steps during movement

to estimate microscopic parameters of the Si-SiO system within the framework of a modified BCF theory. Although the BCF theory is not applicable in its simplest form, it does predict that steps should move more slowly when curved because of changes in the chemical potential, and can not propagate below a certain critical radius which depends on the edge energy and the supersaturation. We observe slowing as steps squeeze between pinning points in figure 5, but do not find the expected straight line relationship between velocity and radius of curvature (although it is hard to estimate step radii accurately given the irregularity of the profiles). This type of analysis on a cleaner, more regular surface would be valuable as it is hard to calculate step energies due to reconstructions which can reduce step energies dramatically [25]; it can also be compared with STM studies of step dynamics which are proving valuable in determining surface terms [26].

A second prediction of the BCF theory is that steps will slow down if closer to one another than a typical diffusion distance, because of the interference between their diffusion fields. In figure 7 the step spacing *decreases* as p_{O_2} increases (from 40μm apart at 2×10^{-6} Torr O_2 to 10μm at 1.5×10^{-5} Torr) suggesting that these distances are greater than diffusion lengths. However the relative immobility of the steep sidewalls surrounding the flat area suggests that the small step spacings here are within the range of diffusion. It can thus be seen that step movement, when viewed within the context of the BCF theory, can indicate the values of parameters such as diffusion length and step energy. However both the complexity of the reaction sequence and the high subsaturations present here mean that this theory must be applied with care.

5.4 Comparison with other dynamical studies

The data we have presented here demonstrate that the etching of silicon by oxygen proceeds by the removal of silicon in double layer steps, 0.31nm in height. Our kinetics results suggest a model of the etching process in which oxygen impinges on the surface, eventually reacting with it and moving into relatively immobile bridging positions. Steps start to nucleate and flow once the oxygen coverage has reached a value below 2 monolayers. Step movement is by evaporation of SiO from step edges with some fraction of the oxygen supplied by diffusion across the surface.

Techniques such as REM and STM potentially have the combination of high spatial resolution at elevated temperatures with the short image acquisition time necessary to carry out comparable dynamical experiments. Both techniques have been used to observe oxygen etching of silicon. Although REM images suffer from severe foreshortening, making it difficult to interpret the morphology observed, Shimizu et al. [19, 27] extracted kinetics data from series of images. Above 500°C at 10^{-8}-10^{-7} Torr, etching proceeded by step movement, as we observe, as well as by the nucleation and growth of hollows in the middle of the terraces. This applied to the Si (001) surface as well [28]. The kinetics of hollow growth were considered in the context of the formation, migration and coalescence of vacancies rather than reacted oxygen species, but otherwise these results are in basic agreement with our own. In our experiments we usually see

nucleation at certain favoured sites but, as mentioned above, on an initially more uniform surface, such as a thick REM specimen, it is likely that nucleation will occur simultaneously at many places on the terrace, provided that the critical oxygen coverage has been reached.

Recently STM images have been acquired at elevated temperatures at sufficient resolution to observe the positions of steps [29]. Etching at 4×10^{-8} Torr and 670°C also occurred by the preferential removal of silicon from step edges, but after the first bilayer had been removed the step edges became more dendritic and the terraces became roughened by bilayer pits. This change in growth mode was attributed to the greater density of defects on the newly formed 7x7 surface than on the surface formed by the initial anneal. This phenomenon may be related to the lower temperature roughening which we have observed and will discuss below. It appears that a balance between diffusion rate of vacancies or adsorbed species, terrace width and defect density accounts for the morphological differences observed during etching.

We expect that further study of oxygen etching under clean, well controlled conditions, using for example STM or LEEM, will yield further quantitative results on the mechanism of this fascinating reaction. However neither of these techniques has the ability to follow the oxidation reaction into silicon planes below the surface. It is this unique ability of TEM which we will now utilise as we explore the low temperature oxidation of silicon.

6. Oxidation

6.1 The initial stages of oxide formation

We have observed the reaction of silicon with oxygen between room temperature and 900°C and at pressures from 10^{-8} Torr to 1atm., as well as oxidation by H_2O at room temperature and pressures of up to 10^{-5} Torr. Images and diffraction patterns obtained during the oxidation reaction show at first sight a very different behaviour from that seen during oxygen etching.

At low temperatures, the initial surface for these oxidation experiments is reconstructed with some oxygen already reacted at bridging positions, as confirmed by electron diffraction [7] and by STM [23]. This 7x7:O surface is stable to oxygen exposures of over 10^5 L O_2 without electron beam irradiation. However if it is irradiated by the electron beam we observe a rapid decrease in order, even for doses much less than 100L, at room temperature [7]. The destruction of the 7x7 structure is confirmed both by the fading of the 7x7 superlattice spots in diffraction, and by the disappearance in forbidden reflection images of triangular features which we believe to be 7x7 $\leftrightarrow$ 1x1 boundaries (figure 4). The $^1/_3$ 422 reflections remain sharp, however, and thus the surface is not undergoing any substantial roughening process.

6.2 Beyond the first monolayer

Forbidden reflection images allow us the unique opportunity to observe the silicon-oxide interface as deeper and deeper atomic layers oxidise progressively at higher doses of oxygen. After

doses above about 10^5 L at room temperature, we observe a fading of the step contrast in irradiated areas of the specimen. This fading is over a much longer timescale than the initial disordering of the 7x7 structure, and represents further oxygen reaction with the 1x1 surface. After even higher doses the step contrast may reappear, but with reversed sense, initially white areas having become black and vice versa. However the 7x7 spots never reappear, and we do not see evidence for any ordering (other than with 1x1 symmetry) in the oxide or the silicon surface layers.

Although at low pressures electron beam irradiation is necessary for this reaction to occur, we have also observed similar contrast reversals at atmospheric pressure without the electron beam. An example is shown in figure 9. The most striking thing about these images is that as the step contrast reverses, the boundaries of the terraces do not move within the resolution of the images (about 2nm). In other words, interface steps do not move either during low pressure, beam induced oxidation or during formation of a native oxide. The same appears to be true for thermal oxidation at 1 atm. and 875°C: after several minutes of oxidation the original step positions are still recognisable (figure 10). The importance of this can not be overemphasised. Native oxidation, thermal oxidation and low temperature beam induced oxidation are clearly terrace reactions, and do not occur preferentially at the surface steps as has previously been assumed; oxidation at steps would randomise the step positions after the reaction of only one atomic layer.

The oxidation reaction with water vapour appears to occur in a similar way to that for oxygen, and we find that contrast reversals occur readily at doses about 400 times lower. Because of the increased speed of this reaction it is possible to observe several cycles of contrast reversals at pressures around 10^{-7} Torr H_2O (figure 11) which can then be used for analysis.

The changes in terrace contrast we observe during oxidation reflect the fact that silicon atoms are being moved substantially, say by more than about 0.05nm, off their crystalline sites as they are incorporated into a (presumably) amorphous oxide. By modeling the contrast levels expected from the remaining silicon, we can derive information about the rate of formation and the nature of the oxide layer.

6.3 The mechanism of oxidation

During the formation of SiO_2, oxygen or water molecules diffuse through the growing oxide film and react at (or near) the silicon-oxide interface. It is important to emphasise that because we see no evidence for step movement during oxidation, this interfacial reaction must proceed by attack of the terraces rather than the steps at the silicon-oxide interface. Attack at steps appears to have been implicitly assumed in oxidation theories because it provides a mechanism to relieve some of the stress caused by the large volume expansion, about 45%, on forming SiO_2 from Si. To account for the immobility of bilayer steps during the reaction, we suggest that oxidation occurs one monolayer at a time, with single planes of atoms not reacting until the layers above are (almost) completely reacted. We will discuss this point in more detail below.

More detail can be inferred about the mechanism of this layer-by-layer oxidation process by measuring the contrast levels from terraces during oxidation (figure 12a). An important qualitative observation is the fact that the intensity levels return to high values at certain times. We expect the average intensity of a partially oxidised (i.e. rough) terrace to depend on the fraction of oxidised sites, and we can model intensity levels from rough interfaces as an incoherent summation of levels from the neighbouring silicon thicknesses. We therefore expect contrast maxima to occur for atomically flat interfaces. The fact that there are strong experimental contrast maxima suggests that at these points an integral number of atomic layers have been oxidised, returning a given terrace to its original atomically flat configuration. Thus it appears that oxidation occurs uniformly, one layer at a time, with a lower layer generally not reacting until the upper layer is completely, or almost completely, reacted. A supporting observation is that random attack of silicon bonds would lead eventually to roughening of the silicon-oxide interface, giving it a half-width proportional to the square root of the oxide thickness, whereas it has been known for some time that the interface is very sharp even after hundreds of nanometers of thermal oxidation [30, 31] (admittedly often with a post oxidation anneal).

We have thus considered two possible terrace attack modes for the oxidation: firstly that "bilayer units" (e.g. A+b in figure 3a) are reacted at once (or in quick succession) as oxygen arrives at the surface, and secondly that the surface reacts one *monolayer* (a or A) at a time, with the second monolayer not reacting until the first is completely oxidised. The essential difference between these models is that the surface returns to atomic level flatness after every monolayer in the second model but only every bilayer in the first (figure 13). We can distinguish between these models by comparing measured contrast levels with those calculated from simulations. In these simulations we ignore the presence of the oxide film, assuming that it does not scatter preferentially into the $^{1}/_{3}$ 422 positions but only contributes a background intensity. Computer simulations for the two models are different at most specimen thicknesses and favour the second scenario for the three data sets we have analysed (for example in figure 12b). However, we prefer not to rely entirely on the matching of computer simulations, mainly because the specimen thickness is not accurately known in these experiments and this may lead to ambiguity in the results. Instead, we support the suggestion of a monolayer reaction with several other points.

One of the most compelling arguments in its favour is that this mechanism provides a natural explanation of the immobility of bilayer interface steps during oxidation. At the intermediate stages of oxidising a bilayer in figure 13a there is nothing special about the site of the original surface step, and step positions will thus drift during oxidation (although they will not become randomised as fast as in a step edge mechanism). To exclude this possibility, our examination of the growth of thick thermal oxides does not suggest a drift in the position of surface steps.

As a mechanism to encourage layer-by-layer oxidation by preventing attack below the uppermost layer, we suggest that Si-Si bonds may be oxidised preferentially if one of the silicon atoms already has an Si-O bond or a dangling bond. This appears to be the case in the reaction of oxygen with the *backbonds* of the adatoms of the 7x7 structure [7]. Asymmetrically bonded silicon atoms are polarised due to the electronegativity of oxygen, and this may be particularly important in enhancing their reaction with H_2O molecules (or OH fragments) as happens during water vapour oxidation.

An interesting feature of this model is that as silicon is removed in monolayers, the shuffle and glide terminations alternate. This is in contrast to the removal of bilayer units at once (or in quick succession) during etching. In the latter case the large energy difference between the two terminations may dominate the reaction kinetics; when the surface is covered by an oxide, however, the dangling bonds are saturated and this energy difference is probably much reduced.

Finally, note that a strong correlation of atomic positions in the oxide with the underlying silicon lattice could modify the overall intensity levels we calculate, although not the way these levels change as silicon is removed. (The possibility that the reaction rate is not uniform, particularly with regard to the times for the two different monolayers A and a, can also affect the match of simulations with data.) More detailed modeling would be required to detect crystalline structure in the oxide. However any crystalline oxide phase must be present in low coverage (<10%) or have one of a restricted range of structures in order to leave no detectable trace in the diffraction patterns. We thus envisage an abrupt crystalline - amorphous change at the interface. Furthermore, the layer-by-layer growth we propose leads naturally to a stoichiometry of SiO_2 within a monolayer of the interface, in agreement with some high spatial resolution, compositionally sensitive results [32, 33].

6.4 Comparison with other oxidation models

As mentioned above, a large volume expansion is associated with silicon oxidation and this is likely to cause high stresses near the silicon-oxide interface. We suggest that stress is more important than has previously been supposed, because we can discount the suggestion that oxidation at step edges (or at jogs in steps) will reduce the strain introduced into the silica near the interface [34]. Several oxidation models include the effects of stress but few, notably the reactive layer model of Stoneham et al. [35], also address the atomic scale structure of the silicon-oxide interface.

In this model, oxidation occurs at the outer surface of a reactive layer, stabilised between the silicon and the growing oxide by strain. The structure of the reactive layer is not specified, but transport through it is supposed to be by silicon interstitials or oxygen vacancies, rather than by O_2 molecules as occurs through the SiO_2 layer; several transport mechanisms were discussed by Mott et al. [36]. The results of the present study are consistent with the reactive layer model but with one

important reservation. Detailed modeling of stress levels around steps [37] suggests that it is overwhelmingly likely that silicon interstitials would be emitted at steps rather than from terraces. Any oxidation mechanism which relies on the diffusion of silicon interstitials is thus also very likely to involve step movement. We therefore do not feel that Si interstitials can be the species which diffuse through the reactive layer; instead we suggest the diffusion of another species such as an oxygen vacancy, as in the model of Robertson [38], to account for the isotope results addressed by the reactive layer model for the initial stages of oxidation.

6.5 Surface morphology and the roughening régime

The immobility of interface steps is of particular significance to device processing, because it suggests that the original surface morphology is preserved during oxidation so that it is important to start with a flat surface. The growth and annealing of a thick sacrificial oxide is conventionally used to remove damaged surface regions and contamination during device processing. The flat interface created by this process presumably also contributes to an improvement in the quality of subsequently formed silicon-oxide interfaces.

In this context it is known that exposure of the surface to conditions within the etching régime prior to oxide growth reduces the quality of MOS devices [39]. This has naturally been assumed to be due to roughening of the surface associated with the etching reaction. Our experiments have shown that etching does not necessarily roughen the surface and may even smooth it (particularly the (111) surface). Instead we suggest that the roughening observed in these studies may occur as the surface crosses the etching-oxidation boundary. We find unusual behaviour, both in diffraction and in imaging, over a small range of temperature and pressure near this boundary (figure 1). In diffraction, we see distinctive ringlike features around the $^1/_3$ 422 reflections (figure 14). By considering the tilt of the reciprocal lattice rods which generate the $^1/_3$ 422 spots, we ascribe these to roughening of the surface with a preferred length scale of around 5nm. In FB images the step contrast disappears and is replaced by a uniform speckled appearance. Where the 7x7 reconstruction is seen with the rings, as in figure 14, the surface is inhomogeneous with some areas already roughened and others still flat. The roughness disappears and the 7x7 spots reappear over a few minutes once the oxygen pressure is reduced to bring the surface into the etching régime. We believe that these phenomena are due to competition between the etching and oxidation reactions, with small areas of oxide forming and locally protecting the underlying silicon from etching (micromasking). This inhomogeneous reaction may be promoted by the presence of contamination on the surface hindering the flow of steps; another possibility, suggested by STM [29], is an increased density of defects on 7x7 surfaces formed at low temperature which may change the nucleation opportunities for steps. Silicon surfaces are likely to pass briefly through this roughening régime during high temperature cleaning to desorb an oxide, and the condition of the surface (oxide thickness, contamination, defect density, etc.) determines whether macroscopic

roughness, as observed by Smith and Ghidini [3] and Offenberg et al. [39], or smaller scale asperities form.

6.6 Electron beam effects during *in situ* studies

To summarise our results, a combination of diffraction and imaging techniques have shown that the double steps present on the clean silicon (111) surface do not take part in the oxidation reaction, which instead proceeds by an attack on the terraces. We believe that oxidation occurs one monolayer at a time with each monolayer reacting completely before the next is attacked.

We were able to carry out our most detailed study of this oxidation mechanism for the case of low temperature, low pressure oxidation. It is known that the oxidation process under these conditions is strongly influenced by external excitation. Irradiation by low or high energy electrons [7, 22, 40, 41] or x-rays [22] is necessary to enable oxidation to proceed beyond the initial stage in which molecular oxygen is adsorbed on the surface. Presumably the electron beam used in our experiments creates electron-hole pairs in the bulk which can dissociate oxygen molecules at the surface at low temperature [21]. However we observed no beam induced effects during etching experiments. At higher temperatures the transformation from a molecular precursor to a bonded state is easier and the effect of the electron beam should therefore be much less significant; the reaction can proceed beyond the first monolayer without external stimulation. These considerations suggest that the effect of the beam may simply be to enhance the oxidation rate at low temperature without causing a fundamental change in the mechanism. This gives us confidence in extrapolating our analysis of low pressure oxidation to other régimes, especially given the result that native and thermal oxidation also proceed via a terrace process.

7 Summary

We have observed the behaviour of terraces and steps dynamically during oxygen etching, native oxidation, thermal oxidation and electron beam-induced oxidation at low pressures of H_2O and O_2. We propose that oxidation occurs monolayer by monolayer at terraces with one layer fully reacted before the next begins, a mechanism which does not favour the movement of silicon interstitials through a reactive layer and which suggests an abrupt crystalline-amorphous transition at the interface. A fascinating contrast is provided by oxygen etching; this is also a terrace reaction but is followed by an evaporative process from surface steps. At the boundary between these two régimes a roughening transition occurs.

The possibilities of an oxidation study where sub-monolayer accuracy can be achieved in measuring the progress of the reaction are very exciting. Detailed observations of oxide thickness, interface structure and the behaviour of steps allow us to distinguish between different models for silicon oxidation. In further studies, we hope to isolate the single silicon surface in an oxidising environment by forming a protective silicide on one surface of the specimen. As we have not

covered the pressure and temperature range addressed by most oxidation models we plan to obtain further results at higher pressure and temperatures. We also intend to examine the Si(100) surface, on which steps can be imaged, although more weakly, using (011) forbidden reflections.

Observations of the behaviour of terraces and individual steps allow us to follow changes in surface and interface morphology during dynamical experiments, and we are confident that the technique we have described here will find many other applications in the study of the atomic scale chemistry of crystal growth, adsorbates and surface defects.

Acknowledgements

We would like to acknowledge the valuable help of D. Bahnck and M. L. McDonald. This work was partially supported by the Director, Office of Energy Research, Office of Basic Energy Sciences, U. S. Department of Energy under contracts Nos. DE AC-03-76SF00098 and DE FG-02-91ER45439.

References

1. F. M. Ross and J. M. Gibson, Phys. Rev. Lett. **68** (1992), 1782
2. J. Lander and J. Morrison, J. Appl. Phys. **33** (1962), 2089
3. F. Smith and G. Ghidini, J. Electrochem. Soc. **129** (1982), 1300
4. M. L. McDonald, J. M. Gibson and F. C. Unterwald, Rev. Sci. Instr. **60** (1989), 700
5. J. M. Gibson, M. Y. Lanzerotti and V. Elser, Appl. Phys. Lett. **55** (1989), 1394
6. K. Takayanagi, Y. Tanishiro, S. Takahashi and M. Takahashi, Surf. Sci. **164** (1985), 367
7. J. M. Gibson, Surf. Sci. **239** (1990), L531
8. D. Cherns, Phil. Mag. **30** (1974), 549
9. J. C. Spence, Ultramic. **11** (1983), 117
10. A. Ourmazd, G. R. Anstis and P. B. Hirsch, Phil. Mag. **48** (1983), 139
11. J. M. Cowley and A. F. Moodie, Proc. Phys. Soc. **76** (1960), 378
12. W. Telieps and E. Bauer, Surf. Sci. **162** (1985), 163
13. R. D. Twesten and J. M. Gibson, submitted to Ultramic. (1993)
14. G. W. Rubloff, J. Vac. Sci. and Tech. A **8** (1990), 1857
15. F. M. Ross and J. M. Gibson, in *Atomic Layer Growth and Processing*, edited by T. F. Kuech, P. D. Dapkus and Y. Aoyagi, Mat. Res. Soc. Proc. **222** (1991), 219
16. W. K. Burton, N. Cabrera and F. C. Frank, Phil. Trans. Roy. Soc. **243** (1951), 299
17. R. E. Schlier and H. E. Farnsworth, J. Chem. Phys. **30** (1959), 917
18. C. Gelain, A. Cassuto and P. Le Goff, Oxid. Metals **3** (1971), 139
19. N. Shimizu, Y. Tanishiro, K. Takayanagi and K. Yagi, Surf. Sci. **191** (1987), 28
20. H. Ibach, H. D. Bruchmann and H. Wagner, Appl. Phys. A **29** (1982), 113
21. P. Morgen, U. Höfer, W. Wurth and E. Umbach, Phys. Rev. B **39** (1989), 3720
22. U. Höfer, P. Morgen, W. Wurth and E. Umbach, Phys. Rev. B **40** (1989), 1130
23. I.-W. Lyo, Ph. Avouris, B. Schubert and R. Hoffman, J. Phys. Chem. **94** (1990), 4400
24. J. P. Pelz and R. H. Koch, J. Vac. Sci. Tech. A **9** (1991), 775
25. J. E. Griffith and G. P. Kochanski, Crit. Rev. Solid State and Mater. Sci. **16** (1990), 255, and references therein
26. M. B. Webb, F. K. Men, B. S. Swartzentruber, R. Kariotis and M. G. Lagally, Surf. Sci. **242** (1991), 23
27. N. Shimizu, Y. Tanishiro, K. Kobayashi, K. Takayanagi and K. Yagi, Ultramic. **18** (1985), 453
28. H. Kahata and K. Yagi, Surf. Sci. **220** (1989), 131
29. A. Feltz, U. Memmert and R. J. Behm, Chem. Phys. Lett. **192** (1992), 271
30. O. L. Krivanek, T. T. Sheng and D. C. Tsui, Appl. Phys. Lett. **32** (1978), 439
31. C. d'Anterroches, J. Microsc. Spectrosc. Electron. **9** (1984), 147

32. C. R. M. Grovenor and A. Cerezo, J. Appl. Phys. **65** (1989), 5089
33. F. M. Ross and W. M. Stobbs, Phil. Mag. **63** (1991), 1
34. N. F. Mott, Phil. Mag. B **55** (1987), 117
35. A. M. Stoneham, C. R. M. Grovenor and A. Cerezo, Phil. Mag. B **55** (1987), 201
36. N. F. Mott, S. Rigo, F. Rochet and A. M. Stoneham, Phil. Mag. B **60** (1989), 189
37. B. Leroy, Phil. Mag. B **55** (1987), 159
38. J. Robertson, Phil. Mag. B **55** (1987), 673
39. M. Offenberg, M. Liehr and G. W. Rubloff, J. Vac. Sci. Tech. A **9** (1991), 1058
40. P. Collot, G. Gautherin, B. Agius, S. Rigo and F. Rochet, Phil. Mag. B **52** (1985), 1051
41. B. Carrière, J. P. Deville and A. El Maachi, Phil. Mag. B **55** (1987), 721

Figure 1

Summary of imaging and diffraction results observed *in situ*. The symbols indicate distinctive behaviour (see text) in the diffraction pattern or FB image recorded over a timescale of up to an hour, although many of the reactions were much faster. Δ = etching régime, $\times$ = oxidation régime, o = roughening régime. The dotted lines are for guidance only. Also shown is the boundary between oxidation and oxygen etching determined by refs. [2] and [3] (LM and SG respectively).

Figure 2

(a) Diffraction pattern from a silicon foil about 200nm in thickness, oriented near the (111) axis, heated and then cooled to room temperature under UHV. Intense diffraction spots from the bulk silicon structure (1), $^1/_3$ 422 reflections (2) and 7x7 superlattice reflections (3) are visible.

(b) Dark field (FB) image taken using one of the $^1/_3$ 422 diffraction spots indicated in figure 2a. Changes in image contrast indicate a 2ML change in the specimen thickness. Both top and bottom surfaces of the specimen have steps, leading to the cross-hatched appearance in certain regions. Terrace widths in this case are about 100nm. A small objective aperture (5μm) is necessary to obtain a good signal to background ratio in these images, which limits the resolution to about 2nm.

(c) FB image of a specimen cleaned at high temperature then etched by oxygen to reduce the foil thickness. Much larger terrace widths, over a micron, are obtained using this method. The surfaces are clean apart from particles of epitaxial SiC which have formed upon heating and which pin the steps during etching. Near the center of the image two steps, one on each surface, can be seen to cross each other in projection.

Figure 3

(a) The structure of silicon projected in the $(1\bar{1}0)$ direction. We show the hexagonal unit cell (**a**=$^1/_2[1\bar{1}0]$, 0.38nm; **b**=$^1/_2[10\bar{1}]$, 0.38nm; **c**=[111], 0.94nm) which has three pairs of atoms lying on close packed planes labeled a-C. Two possible surface terminations, shuffle and glide, are obtained by cutting either within or between pairs: these differ in the number of dangling bonds per surface atom. A bilayer surface step, as shown, preserves the termination.

(b) A schematic amplitude-phase diagram showing the contributions to the $^1/_3$ 422 reflection from the six layers, calculated at a two-beam condition (Δs=0 for a 220 beam). If an integral number of unit cells is present (i.e. 6n layers), zero intensity will result. If the top and bottom of the specimen can terminate at any layer, amplitudes of 0, 1, 2 and $\sqrt{3}$ are possible. (The side of the triangle is 2 units.) However if we only permit one type of surface layer (A, B, C or a, b, c) the number of intensities is reduced to 0, 2, 2 for the glide and 0, 1, 1 for the shuffle (section 4.2). By considering the 7x7 termination as, for example, 0.5ML of b and 0.5ML of c on an A-type surface

(ignoring the adatoms), this pictorial approach suggests that its expected intensity levels are midway between the shuffle and glide terminations.

Figure 4

(a) A clean (<1.3L O_2 dose) silicon surface at room temperature, and (b) after oxidation for 2.40 minutes in 9.0×10^{-7} Torr O_2 (250L O_2 dose). Three repeating contrast levels are seen in the upper right corner, suggesting that the steps are 2ML in height. The triangles seen initially are probably boundaries between areas having the 7x7 and 1x1 structure; the 1x1 structure is perhaps stabilised at this low temperature by contamination on the surface or by mechanical stress [12]. The disappearance of these boundaries correlates with the fading of the 7x7 reflections during oxidation.

Figure 5

Tracing from successive frames ($^1/_{30}$ second apart) of a video recording showing an individual bilayer step moving across the Si (111) surface at 875±50°C under exposure to 2.8×10^{-6} Torr O_2. The step is pinned by surface obstacles (SiC particles).

Figure 6

(a) Intensity levels of successive terraces, recorded by measuring the brightness of the CRT with a photodiode while playing back the video partly shown in figure 5. Steps sweep across the field of view (which is <0.5cm wide) at a fairly uniform rate of 0.8 per second, each causing a change in intensity. (The transients may be due to the response of the image intensifier; the intensity scale is non-linear.) We show the trace from the last seconds of the experiment, at 875±50°C and about 2×10^{-5} Torr O_2. The foil thickness decreases from right to left until the foil broke at point P at an unknown thickness.

(b) Computer simulations of the intensity of the $^1/_3$ 422 reflection shown for specimens with the shuffle and glide terminations. The specimen thickness increases in 0.31nm steps from left to right. The simulation was done using a multislice calculation including higher order Laue zone (HOLZ) effects [15]. To include these effects, each of the six layers in the hexagonal Si unit cell was simulated using a separate grating in the multislice algorithm. The correct specimen tilt (3.1° from the (111) axis) and accelerating voltage (200kV) are parameters in these calculations. It can be seen that the experimental intensity levels match up with those predicted for the shuffle simulation and not well with the glide if a thickness of 5.3nm is assumed at P.

Figure 7

(a) The rate at which flowing surface steps pass a fixed point, as a function of oxygen pressure

(b) The speed the steps move, measured at three different positions (**b**, **c**, **d**) indicated in figure 5.

Figure 8

Schematic diagram of two possible mechanisms for the etching reaction, with shaded areas representing sites where oxygen has reacted. Oxygen firstly impinges on the terraces. In (a) it reacts with Si only at the exposed atoms at step edges; in (b) the reaction occurs over the whole terrace. Evaporation still occurs preferentially from step edges in this case, but steps can only start to flow as the reacted oxygen coverage approaches 100% because unreacted sites act as pinning centers.

Figure 9

(a) FB image of a clean Si 7x7 surface at 400±50°C; (b) after exposure to 1 atm. pure O_2 at 400±50°C for 20 minutes. A native oxide of thickness 1.0-1.5nm has formed during this time. Although the step contrast has reversed, indicating that oxidation has occurred, every detail of the step distribution is identical in the two images.

Figure 10

FB images (a) before and (b) after thermal oxidation carried out in the microscope at 875±50°C for 10 minutes. We expect about 10nm of oxide to have grown. Some pitting has apparently occurred at the silicon-oxide interface, but the step positions are still recognisable.

Figure 11

Part of a series of FB images showing progressive changes in terrace contrast upon exposure at room temperature to H_2O vapour at 2.5×10^{-7} Torr. Doses are given in Langmuir ($1L=10^{-6}$ Torr seconds).

Figure 12

(a) Grey levels measured by densitometry of the images shown in figure 11. The intensities are normalised to take into account the different overall brightness of the images. The central terrace in figure 11 is assumed to be the lowest (i.e. thinnest).

(b) Calculated intensities for the bilayer and monolayer models at an estimated specimen thickness of 40nm. The multislice algorithm including HOLZ effects was used, and we assumed that both surfaces of the specimen were oxidising at the same rate. At intermediate points we assumed

random attack of unit cells and averaged the intensities. Only one of the three terrace levels is shown for clarity. The others are obtained approximately by translating by 2 monolayers.

Figure 13
Schematic diagrams of (a) the bilayer model and (b) the monolayer model for oxidation of a stepped surface. Letters refer to the atomic planes indicated in figure 3a.

Figure 14
(a) Diffraction pattern of a clean Si 7x7 surface at 600±50°C; (b), (c) after exposure to oxygen at 2×10^{-6} Torr for 4 and 8 minutes. Note the rings around the $^1/_3$ 422 spots and the eventual disappearance of the 7x7 reflections.

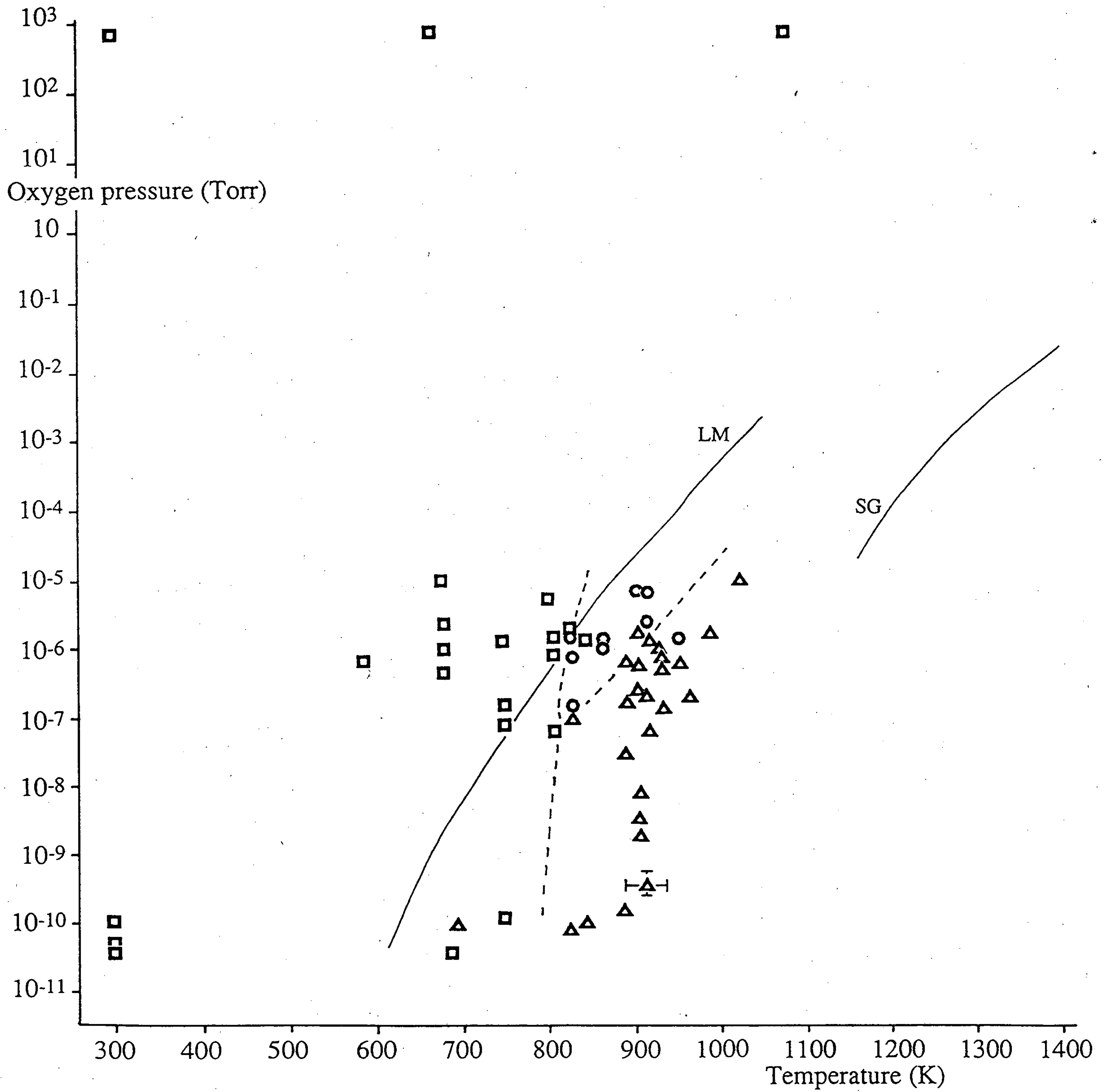

Figure 1 Ross and Gibson

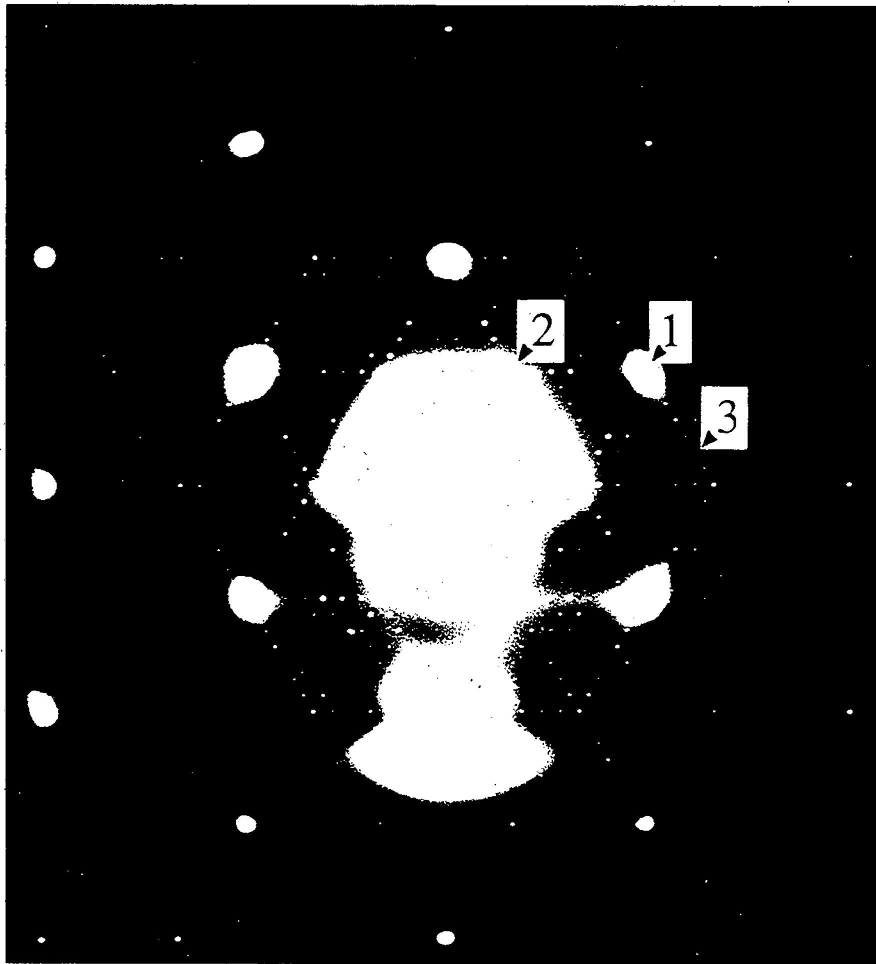

FIGURE 2a: Ross and Gibson

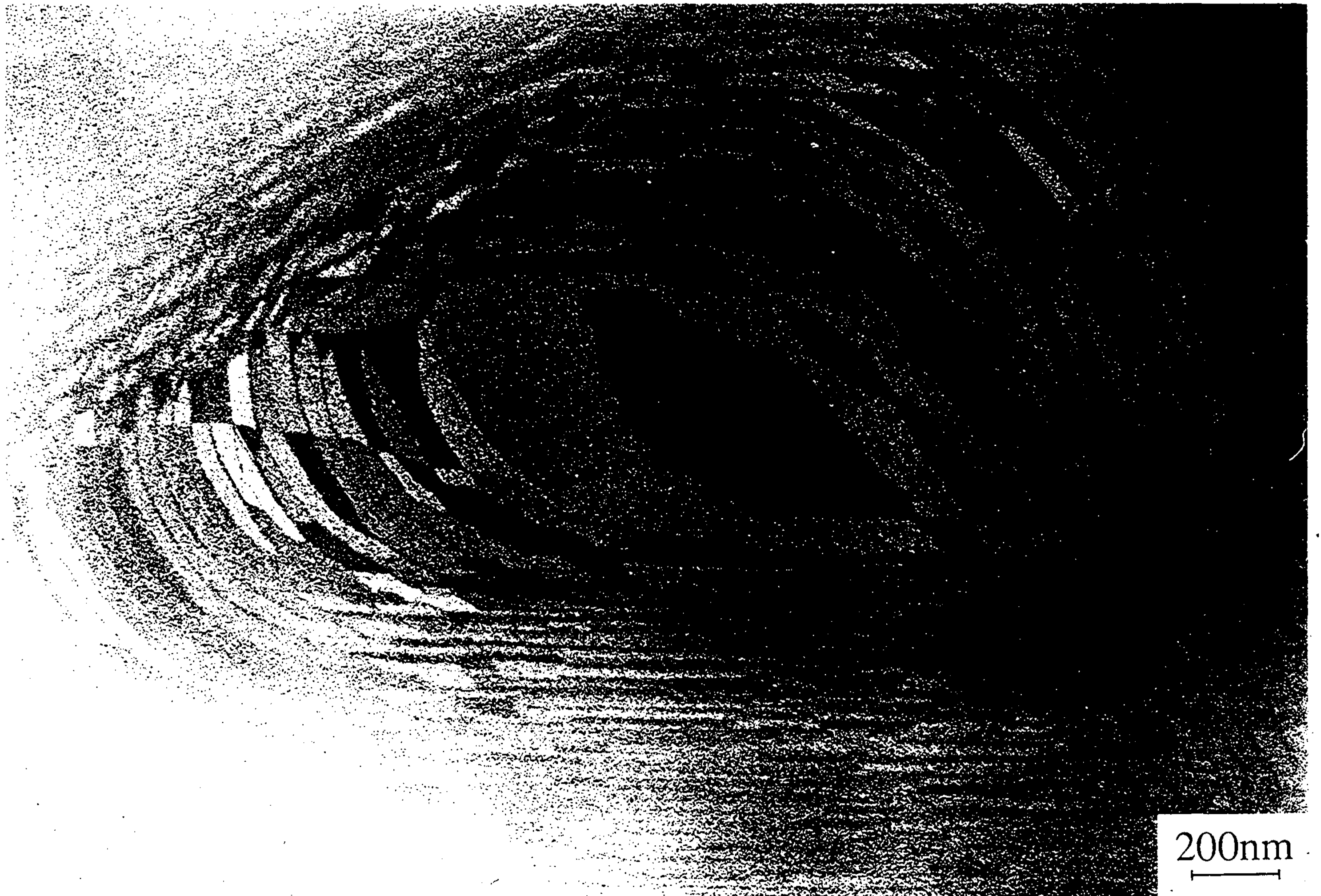

FIGURE 2b: Ross and Gibson

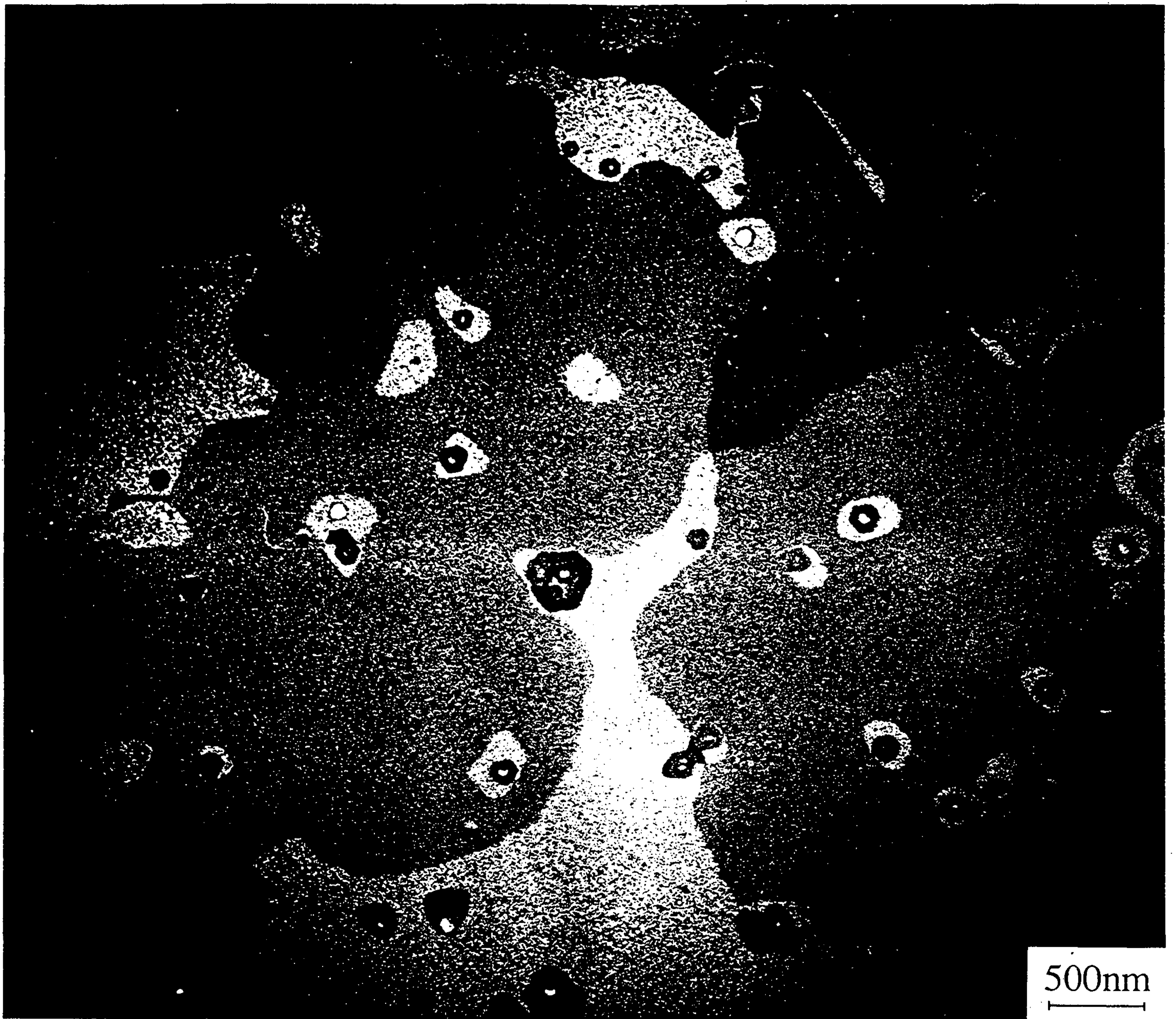

FIGURE 2c: Ross and Gibson

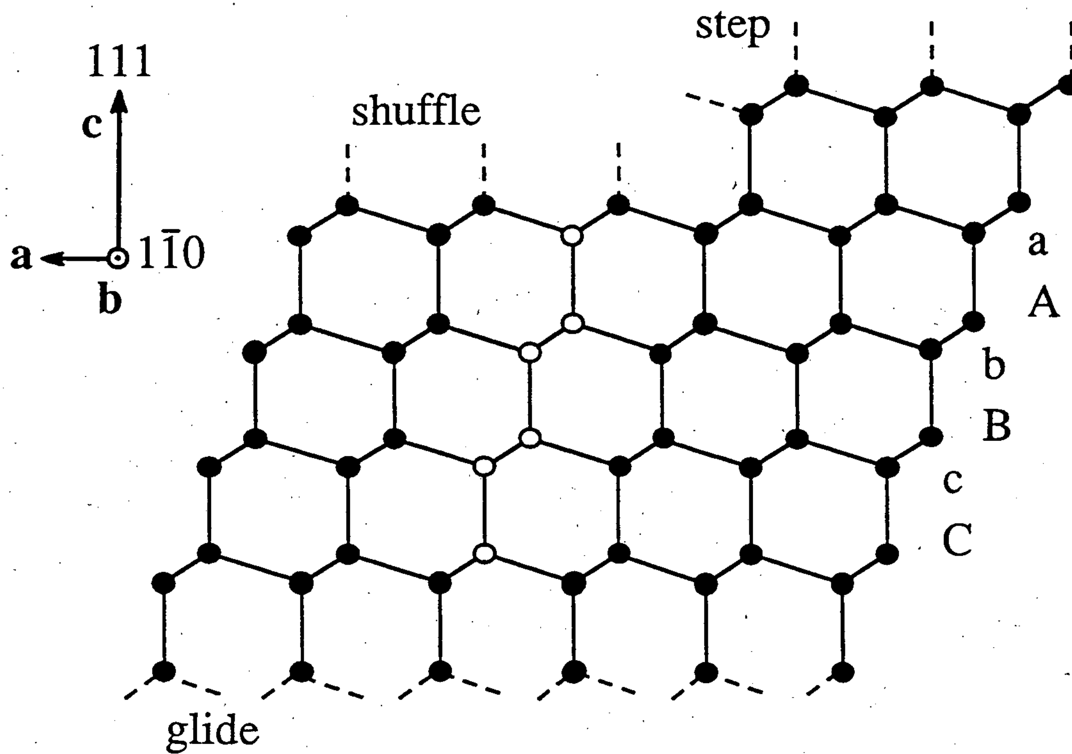

(a)

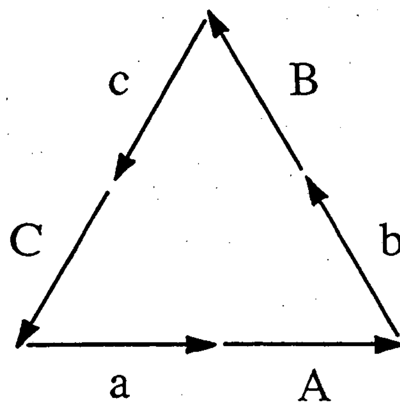

(b)

Figure 3 Ross and Gibson

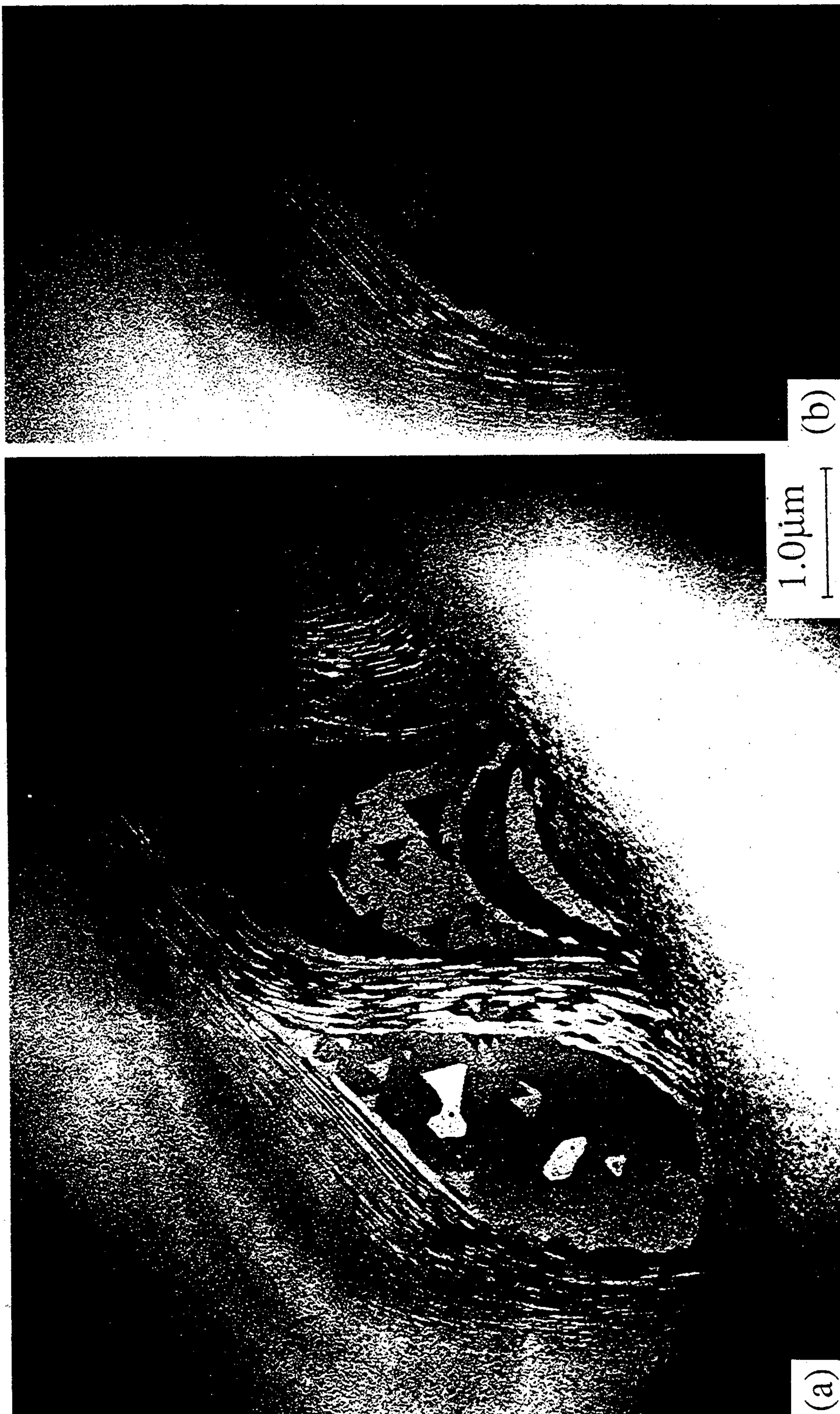

FIGURE 4: Ross and Gibson

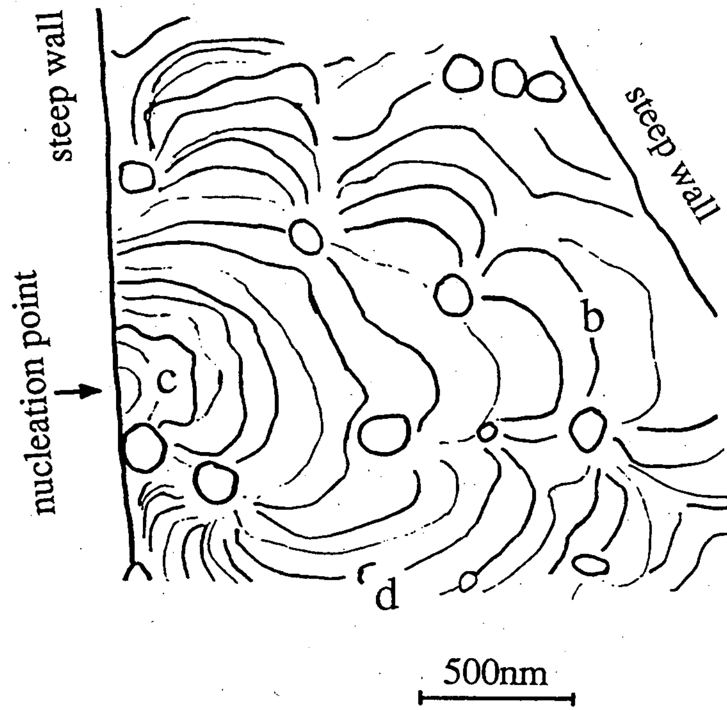

Figure 5 Ross and Gibson

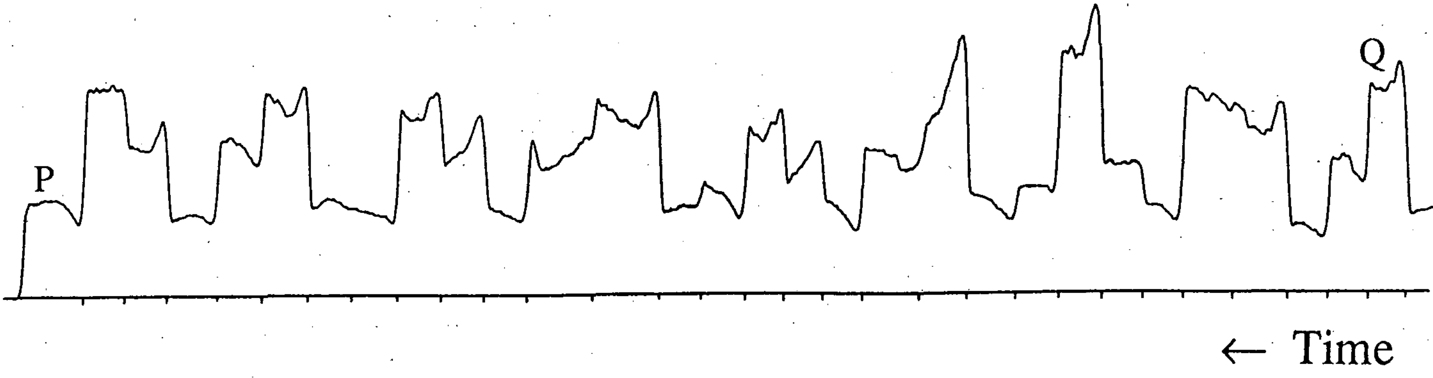

Figure 6 Ross and Gibson

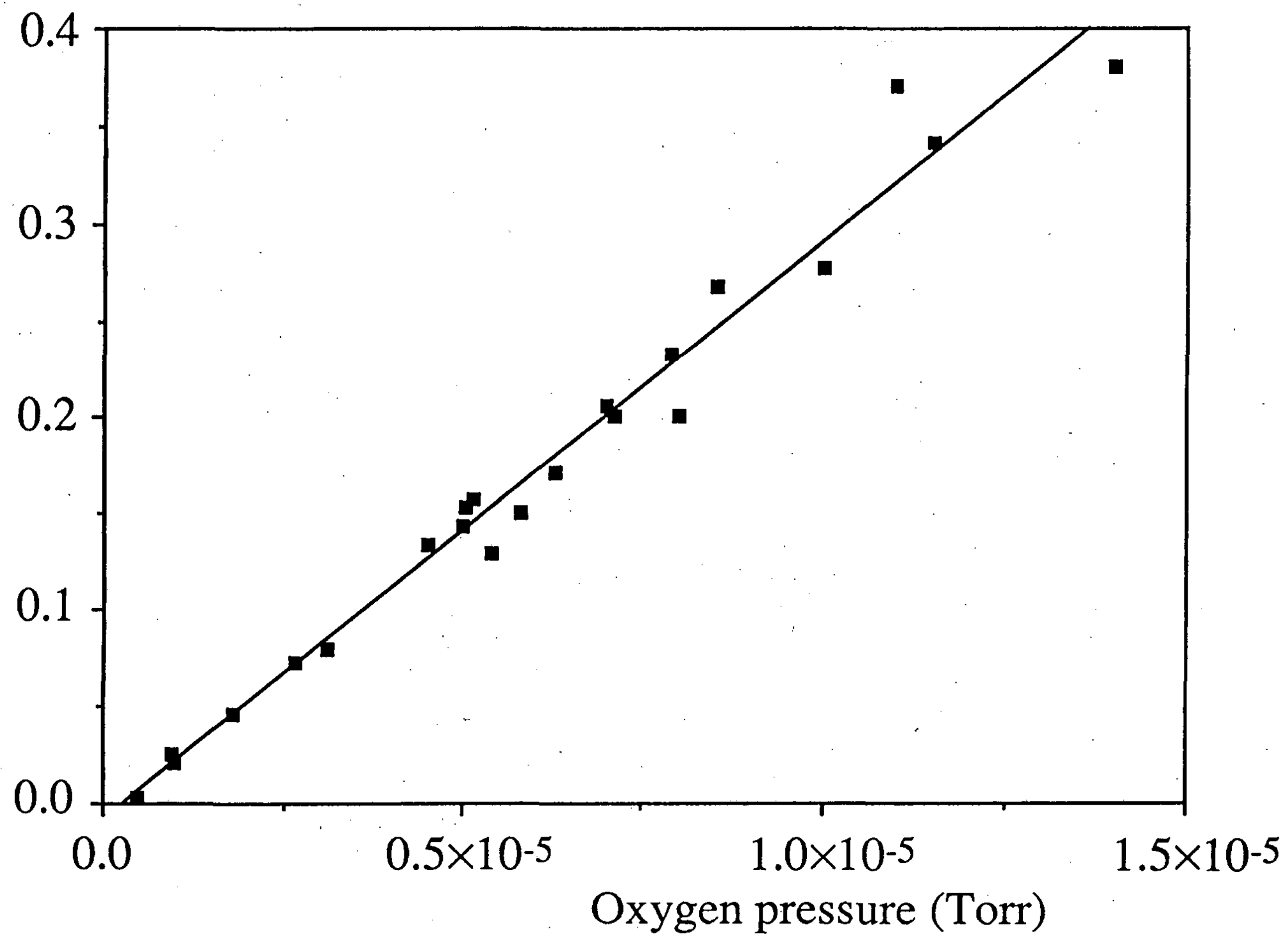

Figure 7a Ross and Gibson

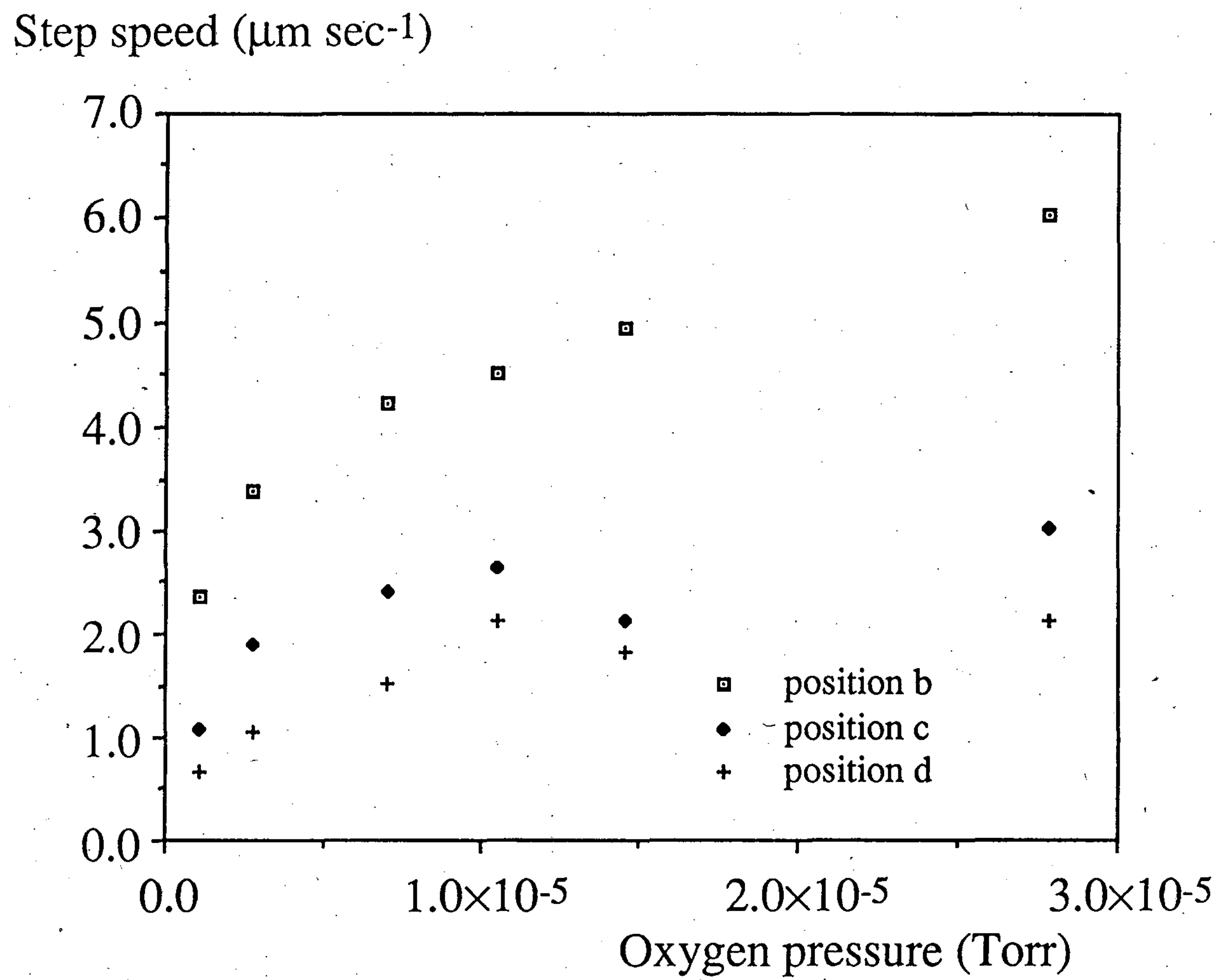

Figure 7b Ross and Gibson

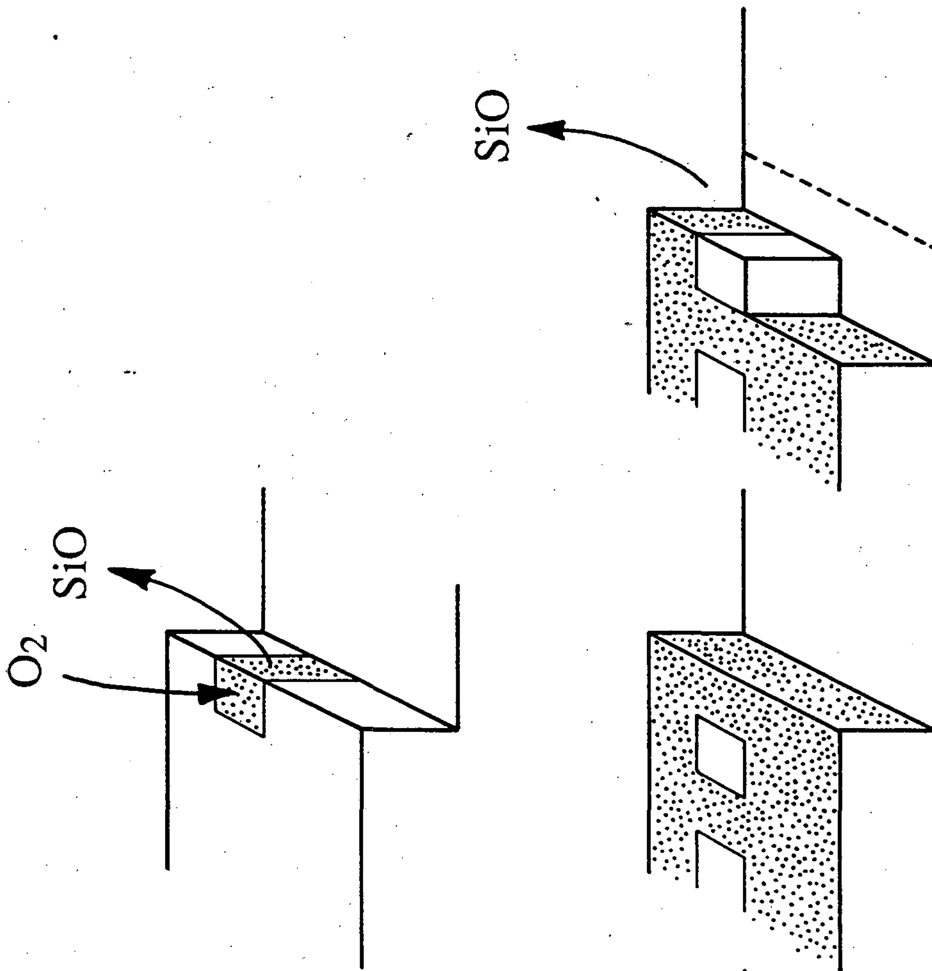

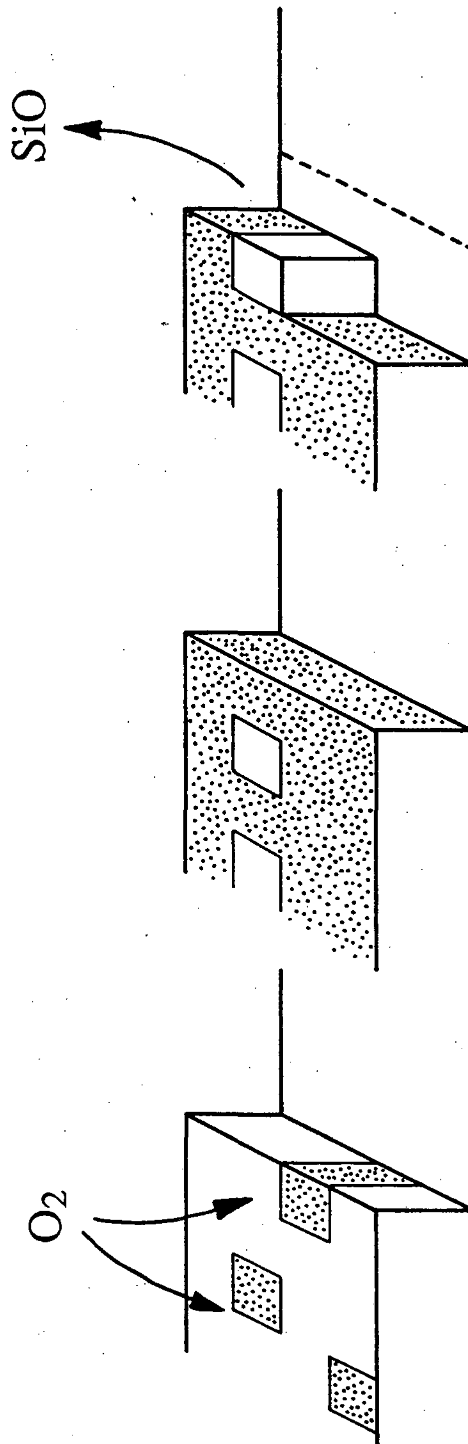

Figure 8 Ross and Gibson

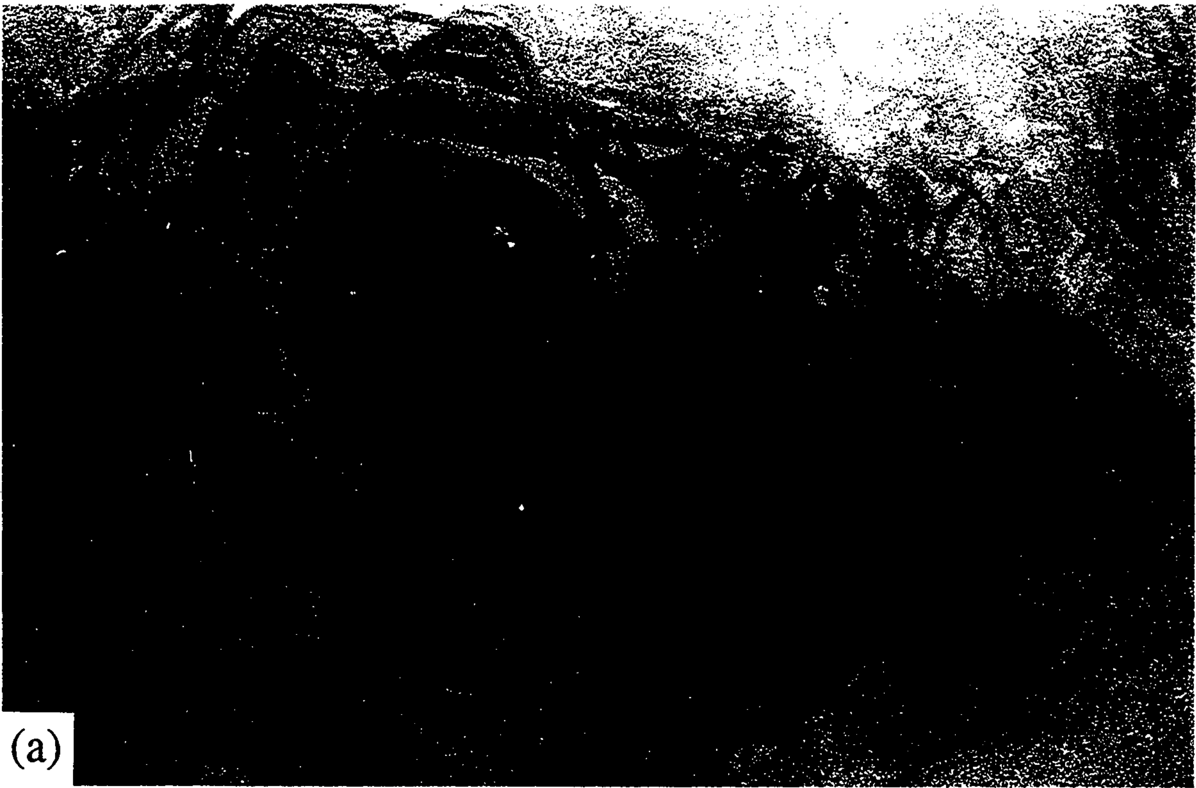

Figure 9 Ross and Gibson

Figure 10 Ross and Gibson

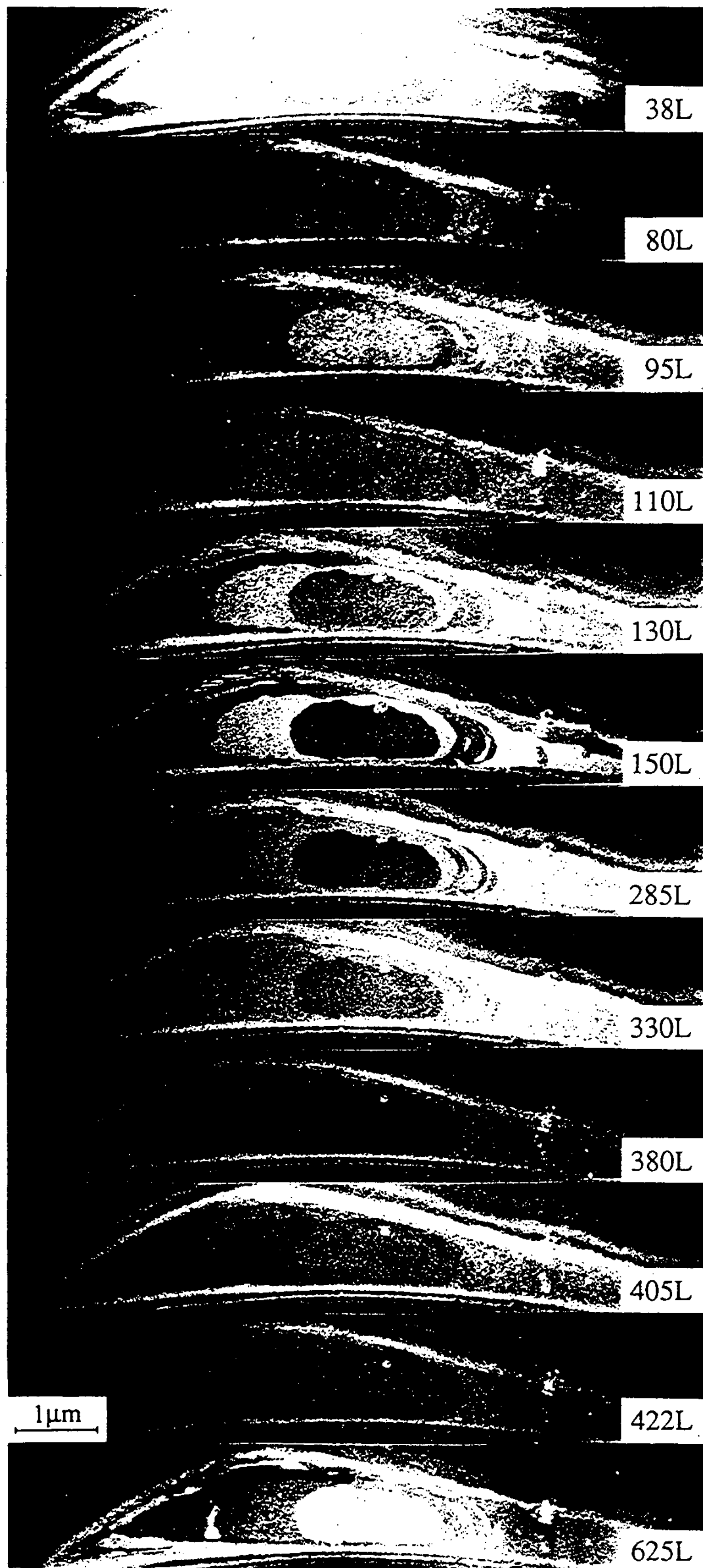

FIGURE 11: Ross and Gibson

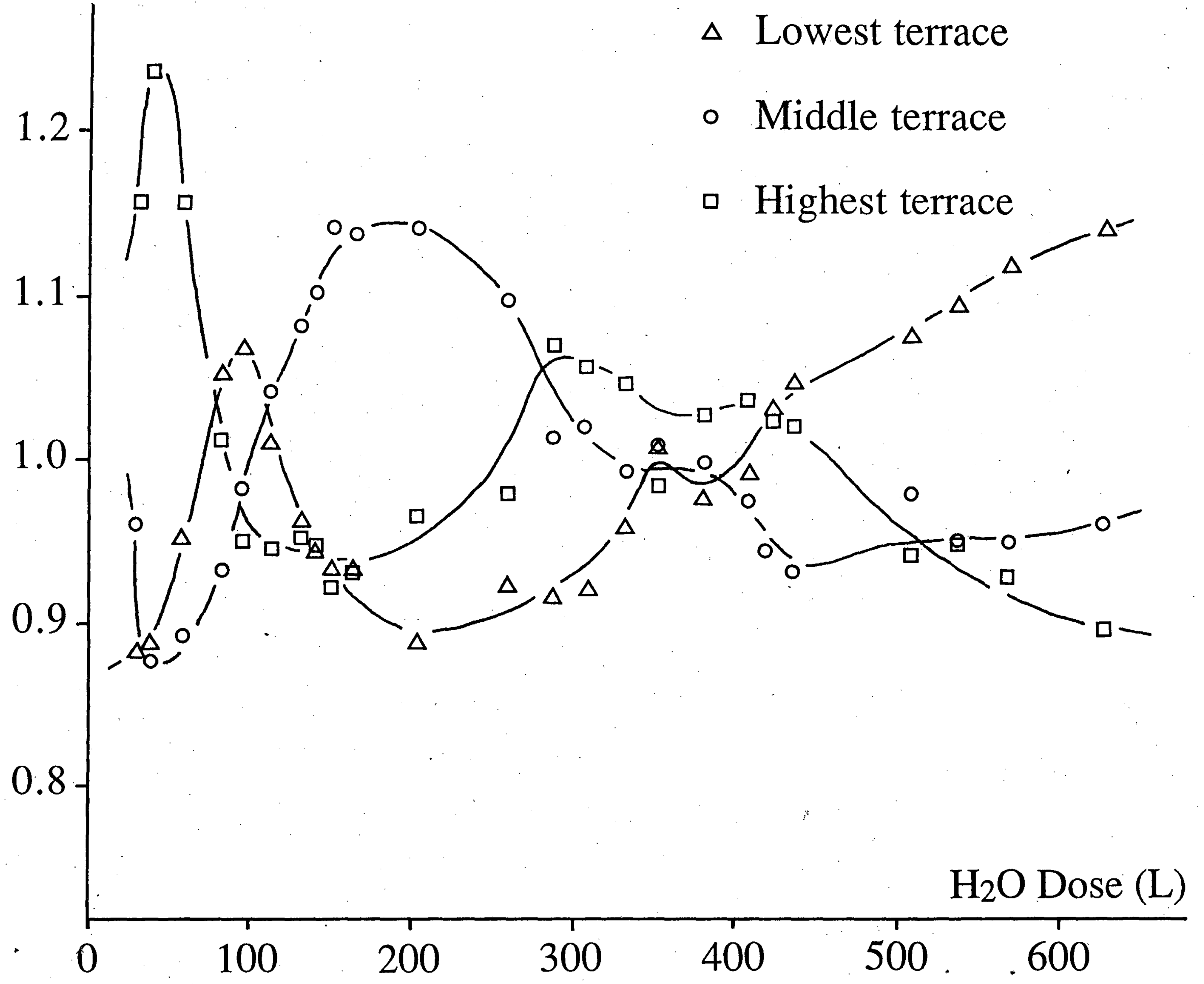

Figure 12a Ross and Gibson

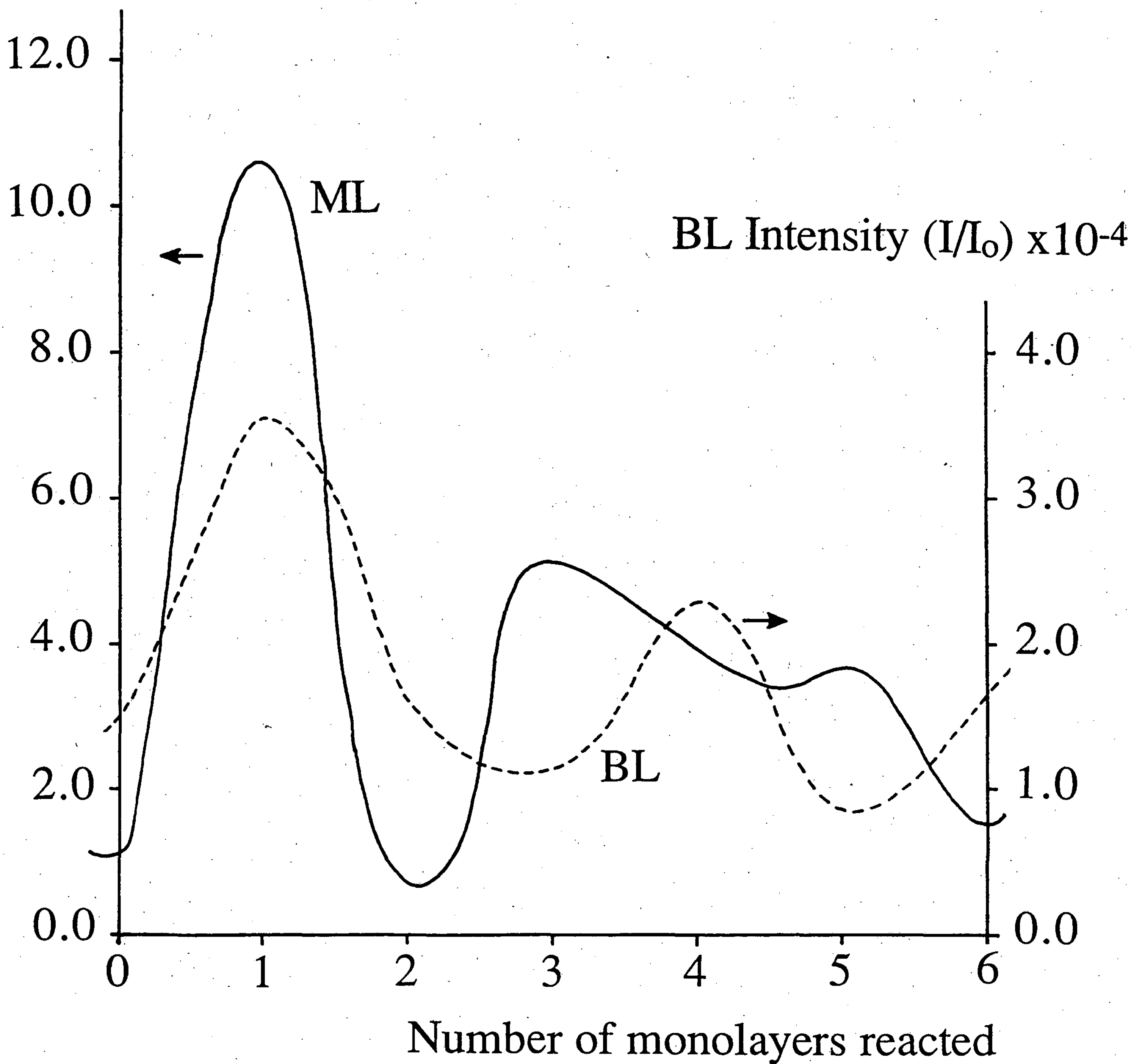

Figure 12b Ross and Gibson

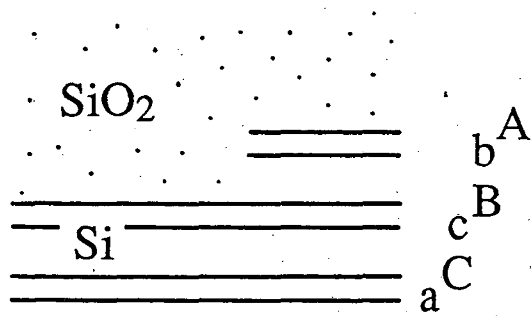

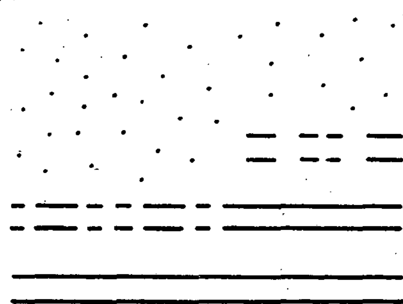

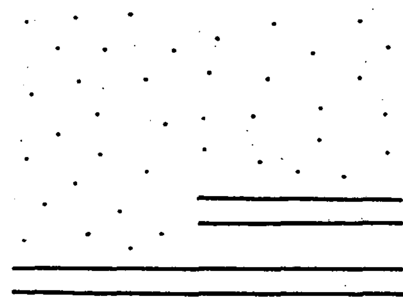

(a)

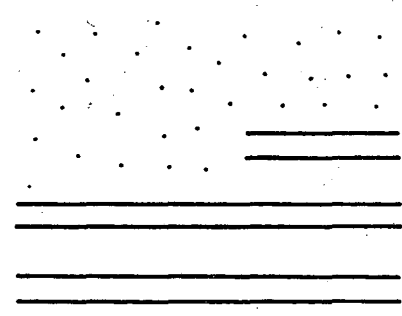

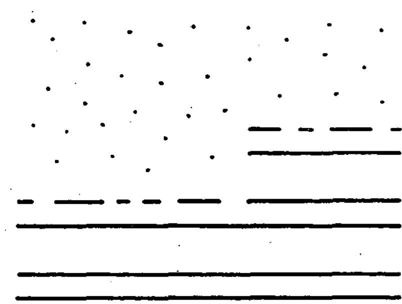

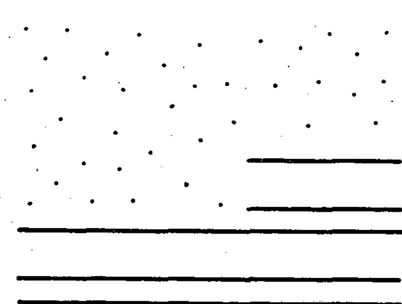

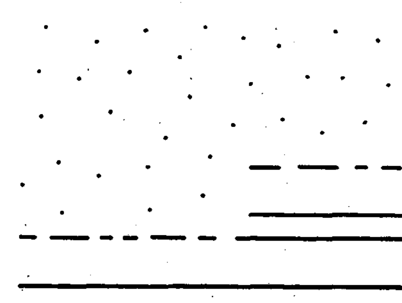

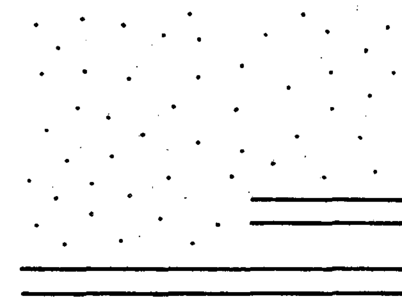

(b)

Figure 13 Ross and Gibson

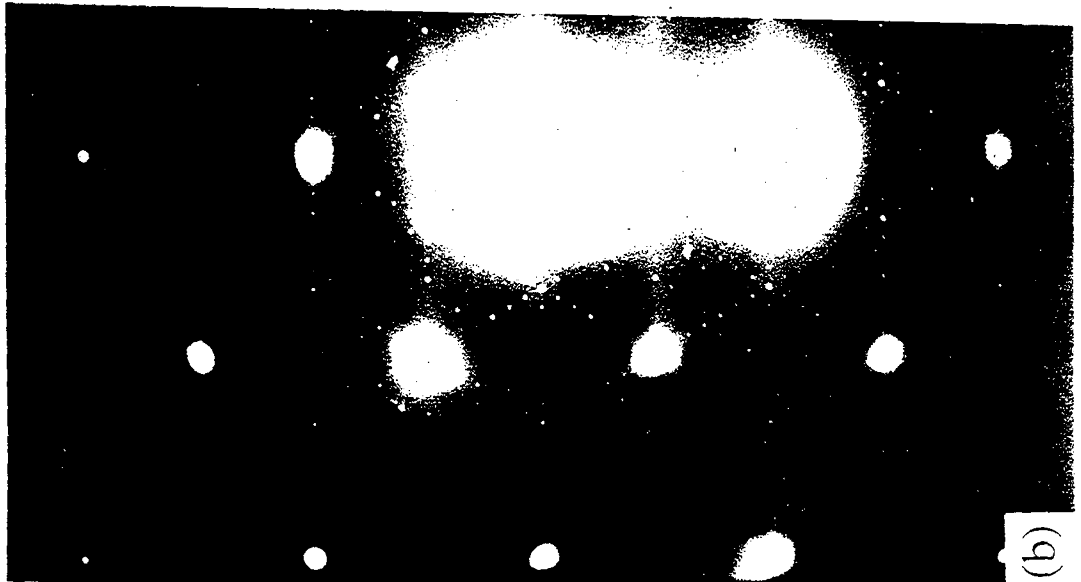
(b)

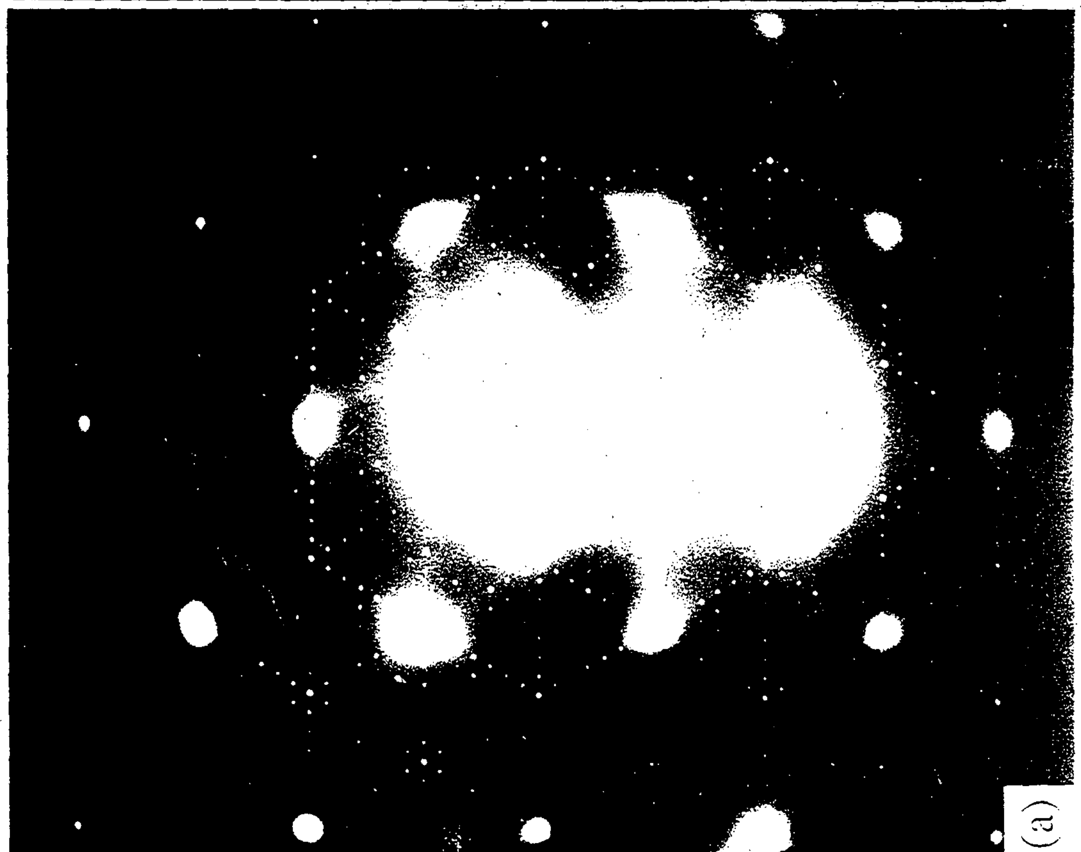
(a)

LAWRENCE BERKELEY LABORATORY
UNIVERSITY OF CALIFORNIA
TECHNICAL INFORMATION DEPARTMENT
BERKELEY, CALIFORNIA 94720